

# Evaluation of hydrogeochemical processes and groundwater quality in the Jhansi district of Bundelkhand region, India

Abhay Kumar Singh · Beenu Raj · Ashwani K. Tiwari · Mukesh K. Mahato

Received: 25 January 2012 / Accepted: 20 December 2012 / Published online: 4 January 2013  
© Springer-Verlag Berlin Heidelberg 2012

**Abstract** A base line study involving analysis of groundwater samples from the Jhansi district were carried out to determine the major and trace element chemistry and to assess the hydrogeochemical processes and water quality for domestic and irrigation uses. Study results show that groundwater is mildly acidic to alkaline in nature and  $\text{HCO}_3^-$ ,  $\text{Cl}^-$ ,  $\text{Ca}^{2+}$ ,  $\text{Na}^+$  and  $\text{Mg}^{2+}$  are the major contributing ions for the dissolved loads. The data plotted on the Gibbs and Piper diagrams reveal that the groundwater chemistry is mainly controlled by rock weathering with secondary contribution from anthropogenic sources. In a majority of the groundwater samples, alkaline earth metals exceed alkalies and weak acid dominate over strong acids. Ca–Mg– $\text{HCO}_3$  is the dominant hydrogeochemical facies in the majority of the groundwater samples. The computed saturation indices demonstrate that groundwater is over-saturated with respect to dolomite and calcite. Kaolinite is the possible mineral that is in equilibrium with the water, implying that the groundwater chemistry favors kaolinite formation. A comparison of groundwater quality parameters in relation to specified limits for drinking water shows that the concentrations of TDS,  $\text{F}^-$ ,  $\text{NO}_3^-$ , total hardness and Fe are exceeding the desirable limits in many water samples. Quality assessment for irrigation uses reveal that the groundwater is of good to suitable category. Higher salinity and residual sodium carbonate values at some sites

restrict the suitability of groundwater and need an adequate drainage and water management plan for the area.

**Keywords** Jhansi district · Groundwater quality · Hydrogeochemical processes · Sodium adsorption ratio · Residual sodium carbonate · Kelley index

## Introduction

Access to safe drinking water remains an urgent necessity, as 30 % of urban and 90 % of the rural Indian population still depends completely on untreated surface or groundwater resources (Kumar et al. 2005). While access to drinking water in India has increased over the past decade, the tremendous adverse impact of unsafe water for health continues. It is estimated that about 21 % of the communicable diseases in India are water born (Bradon and Homman 1995). Though recent years shift in usage from surface water to groundwater has controlled microbiological problems in rural India to a certain extent, but the same has led to newer problems of fluorosis, arsenicosis and salinity due to overexploitation of groundwater. Excess iron is an endemic water quality problem in many part of the India. About 17 Indian states were affected by problems of fluorosis in 2002, which has now been extended to more than 20 states, indicating that endemic fluorosis has emerged as one of the most alarming public health problems in the country (Choubisa 2001; Susheela et al. 1993; Susheela 1999; Teotia and Teotia 1984). Deteriorating quality of the available water resources and availability of potable water is being recognized as a major crisis in many parts of the India (Subramanian 2000; Singh et al. 2011). The overdependency on groundwater has led to 66 million people in 22 states at risk due to excessive fluoride and

A. K. Singh (✉) · B. Raj · A. K. Tiwari · M. K. Mahato  
CSIR-Central Institute of Mining and Fuel Research,  
Dhanbad 826 015, India  
e-mail: singhak.cimfr@gmail.com

B. Raj  
IEDS, Bundelkhand University, Jhansi, UP, India

around 10 million at risk due to arsenic in six states (Ghosh 2007). In addition, there are problems due to excessive salinity in the coastal areas and iron, nitrate and hardness in other parts of the India (Srikanth 2009).

The Bundelkhand region occupies an almost 70,000 km<sup>2</sup> area in central India, covering seven districts of south-western Uttar Pradesh (Jhansi, Lalitpur, Jalaun, Hamirpur, Banda, Mahoba, Chitrakoot) and six districts (Sagar, Chhatarpur, Tikamgarh, Panna, Damoh and Datia) of northeastern Madhya Pradesh (Fig. 1). Apart from its rich cultural heritage, the Bundelkhand region is also known for its socio-economic backwardness. Most districts of the Bundelkhand region have the lowest levels of per capita income and are identified as poorest districts of the country by the Planning Commission. For most of the year, the residents of Bundelkhand experience acute scarcity of water for agricultural, industrial and domestic uses. Water sources are varied and often seasonal; ranging from ponds, tanks, lakes and streams to open wells, bore wells and irrigation canals. Local inhabitants rely primarily on subsistence rainfed single crop agriculture and small-scale livestock production for their livelihood. The region is not only suffering from the availability of water but the potability of the water is also of great concern. There are reports of high iron, nitrate and fluoride content at some pockets in the Bundelkhand belt, demanding a detailed investigation of the water resources for its better utilization and management (CGWB 2008). The major objective of this study is primarily investigation and interpretation of the groundwater chemistry of Jhansi district for understanding the water–rock interactions and solute acquisition processes that control groundwater composition and to assess groundwater quality for drinking and irrigation purpose.

### Study area

Jhansi district lies in the south western part of the Uttar Pradesh, bounded by latitude 25°07' to 25°57' North and longitude 78°10' to 79°25' East and covering geographical areas of 5,024 km<sup>2</sup>. Jhansi district is bordered on the north by Jalaun, in the east by Hamirpur and Mahoba, south and south-west by Tikamgarh and Lalitpur and on the west by Datia and Bhind districts (Fig. 1). It has eight administrative blocks and total population of the district is around 1,744,907. Groundwater and canals are the main source of water for irrigation and dug wells, tube wells and supply pipelines are the major source of water for drinking uses in the district. Betwa and Dhasan are the major rivers controlling the drainage pattern and the natural slope of the area is in the north and northeast direction. The climate is sub-humid and characterized by a hot dry summer and cold winter. January is the coldest month of the year with the

mean daily maximum and minimum temperature of 24.1 °C and 9.2 °C, respectively. May is the hottest month with mean daily maximum temperature of 42.6 °C and minimum of 28.8 °C. The average annual rainfall of the district is 850 mm and about 91 % of the annual rainfall takes place during the monsoon months of June, July, August and September. Jhansi district lies in the belt of drought prone regions of Uttar Pradesh. The large population (80 %) of the district is living in villages and dependent on agriculture, livestock and forest products. Mining of stones, sand, gravel and building materials represent very low activity and limited employment potentials for reducing dependent on agriculture. The life of the habitants becomes miserable in summer when the water supply source like dug well, tanks, ponds etc. dry up due to failure of monsoon.

The geology of the Jhansi district area is mostly comprised of Bundelkhand Gneissic Complex (BGC) of Archaean Age and Alluvium of Recent Age (Fig. 1). The Bundelkhand Gneissic Complex comprises mainly of 2,500–2,600 Ma old non-foliated granitic rocks with enclaves of gneisses, banded magnetite, calc-silicates and ultramafics (Basu 1986). In addition, there are gneisses, quartz reefs and dykes of basic rocks and tuffaceous serpentine rocks. Dolerite dykes are very common in the BGC and it varies in width, some times attain a width up to 45 m and traceable over 11 km. Dolerite dykes are usually medium grained and dark grayish green in color. They intrude the granites as well quartz reefs and mostly cut across the quartz reefs at right angles. In addition, felsite and porphyry dykes were also reported from area the around Jhansi (Basu 1986). Ultramafic rocks are mainly peridotites, dunites, pyroxenites and gabbro, which are closely associated with metabasic rocks and occur as discrete patches in granites near Jhansi. Quartz and plagioclase feldspar are the essential leucocratic minerals; biotite, chlorite, hornblende, pyroxene and olivine occur as the major ferromagnesian minerals and muscovite, sphene, apatite, zircon and magnetite are the common secondary minerals associated with the rock formations of the area (Mishra and Sharma 1975).

Physiographically, the area can be divided into two units (1) southern Bundelkhand pediplane province and (2) northern highly eroding composite plain province. The northern part of the district is mainly occupied by the alluvium of Quaternary age. The alluvium consisting of mainly fine to coarse sand, gravel, pebble, silt, clay and kankar (calcium carbonate nodule) and attains a maximum thickness of about 60 m. The alluvium together with the underlying weathered zone of granite-gneissic basement forms a more or less homogeneous aquifer system (CGWB 2008). The aquifer thickness varies from 50 to 150 m in unconfined formations and the groundwater in these strata

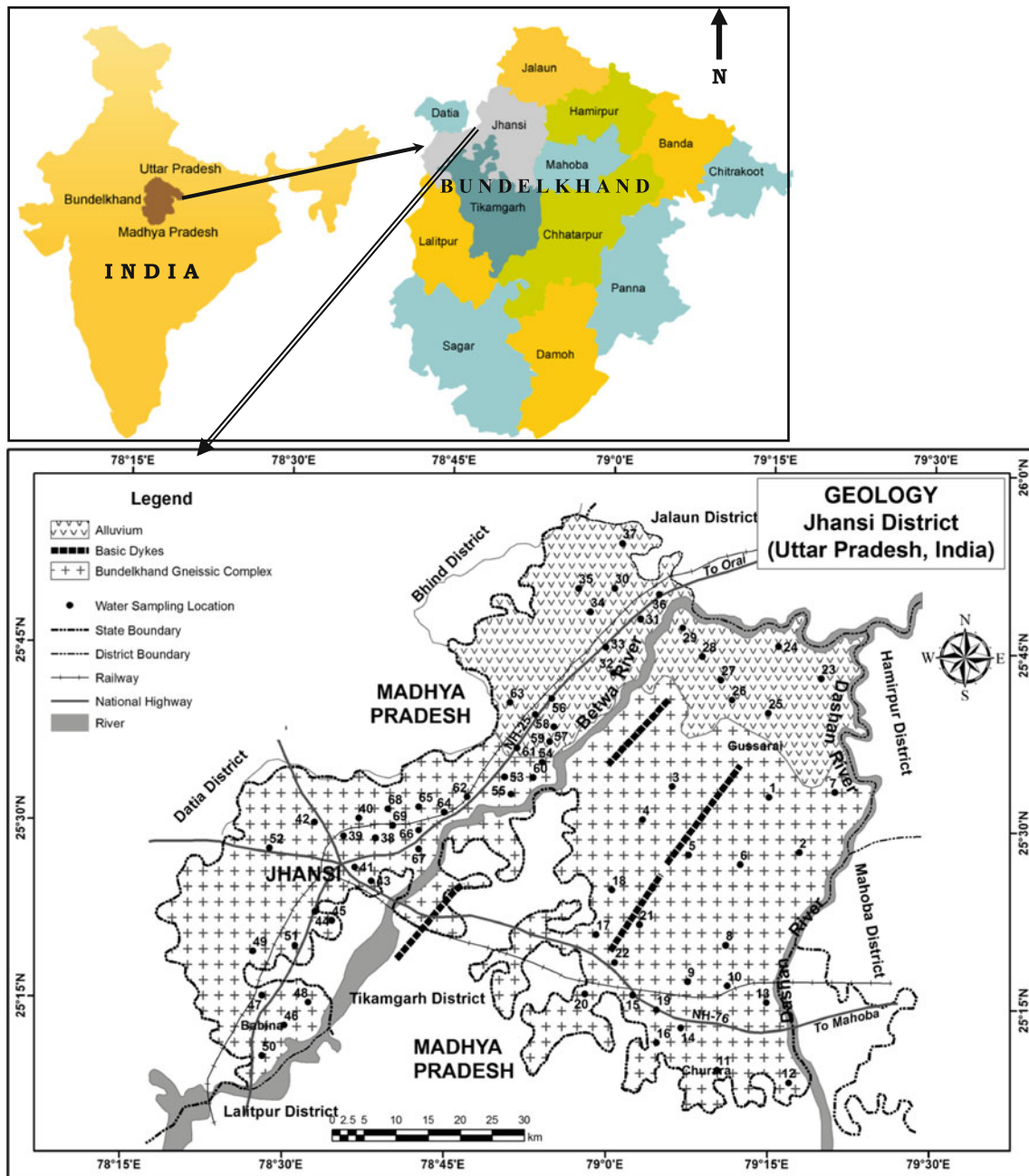


**Fig. 1** Location and geological map of the Jhansi district showing sampling locations

is generally occurs in the upper zone of 40 m and under semi-unconfined conditions at deeper level below 40 m. The northern aquifer system yields moderate quantities of groundwater through dug wells and tube wells. In southern parts of the district, the weathered zone of Bundelkhand granite-gneissic complex and overlying residual soils largely forms the aquifer system. The aquifer system exhibits heterogeneity to some extent due to impervious nature of frequently occurring outcrops, hillocks and linear quartz reefs. This aquifer has an average thickness of about 20–40 m and yield is limited to moderate through dug

wells and tube wells. Groundwater occurs under water table conditions in plains. In the granitic terrain, groundwater occurs in fractures and in fine interstices of the weathered rock material. The depth to water level varies from 5 to 15 mbgl during pre-monsoon. In general, shallow water levels are observed only as patches around Moth and Gursarai, while the western part of the district normally shows water levels between 5 and 10 mbgl. In post-monsoon period, depth to water level varies from 2.47 to 16.07 mbgl. Water level fluctuation varies from 0.85 to 3.65 m. The shallow dug wells are found in canal

command area and the deeper ones are located along the Betwa River. The wells generally meet the domestic and irrigation requirements. Depth of drinking water tube wells varies from 100 to 150 mbgl, while the depth of the dug wells and hand pumps varies from 10 to 20 m and 30 to 50 mbgl, respectively. The yield of tube wells varies from 200 to 600 l pm in hard rock areas (CGWB 2008).

## Methodology

One-liter water samples were collected in pre-washed high-density polyethylene bottles from shallow (dug wells) and deep aquifers (hand pumps) in January 2010 at different locations of the Jhansi district (Fig. 1); and 100 ml of water samples were separately collected and acidified with ultra pure nitric acid for heavy metal analysis. Electrical conductivity (EC) and pH values were measured in the field using a portable conductivity and pH meter (Consort C831). In the laboratory, the water samples were filtered through 0.45  $\mu\text{m}$  Millipore membrane filters to separate suspended particles. Acid titration and molybdosilicate methods were used to determine the concentration of bicarbonate ( $\text{HCO}_3^-$ ) and silica ( $\text{SiO}_2$ ) respectively in water (APHA 1998). Major anions ( $\text{F}^-$ ,  $\text{Cl}^-$ ,  $\text{SO}_4^{2-}$ ,  $\text{NO}_3^-$ ) were analysed on ion chromatograph (Dionex Dx-120) using anions AS12A/AG12 columns coupled to an anion self-regenerating suppressor (ASRS) in recycle mode. Major cations ( $\text{Ca}^{2+}$ ,  $\text{Mg}^{2+}$ ,  $\text{Na}^+$ ,  $\text{K}^+$ ) were measured by Atomic Absorption Spectrophotometer (Varian 680FS) in flame mode after calibrating the instrument with known standards. Three replicates were run for each sample for cation analysis and the instrument was recalibrated after every 15 samples. An overall precision, expressed as percent relative standard deviation (RSD), was obtained below 10 % for the entire samples. Concentration of trace metals in acidified water samples were determined by ICP-MS (Perkin Elmer DRCe). The accuracy of the analysis was checked by analyzing a NIST 1643e water reference standard. The precision obtained in most cases was better than 5 % RSD with comparable accuracy. Overall data reproducibility for anions was within  $\pm 10$  %. Cationic and anionic charge balance ( $<10$  %) is an added proof of the precision of the data. Concentration contour maps were constructed by using ARC GIS-9.2 software to delineate spatial variation of dissolved ions in the groundwater samples.

## Results and discussion

The physico-chemical data for the analysed 69 groundwater samples of the Jhansi district are given in Table 1. The table also shows detailed anion and cation charge

balance in milliequivalent and computed values of chloroalkaline indices (CAI), sodium adsorption ratio (SAR), %Na, residual sodium carbonate (RSC) and Kelley's index (KI). Statistical analyses of the data show that the total cations ( $\text{TZ}^+$ ) and total anions ( $\text{TZ}^-$ ) are coupled by the relation of  $\text{TZ}^+ (\text{meq L}^{-1}) = 1.106 * \text{TZ}^- (\text{meq L}^{-1}) - 1.248$  with a correlation coefficient of 0.98 and the charge differences are within  $\pm 8$  %.

## Groundwater chemistry

The pH of the analysed samples ranges from 6.7 to 8.6 with an average value of 7.5, suggesting mildly acidic to alkaline nature of groundwater (Table 1). Electrical conductivity (EC) measures the salt concentrations of water and provides indication of ionic concentrations. The electrical conductivity of groundwater in the study area varies from 174 to 4,450  $\mu\text{S cm}^{-1}$  with an average value of 852  $\mu\text{S cm}^{-1}$  at 25 °C. Concentration of total dissolved solid (TDS) in the groundwater of the area ranged from 152 to 2,667  $\text{mg L}^{-1}$  with an average value of 673  $\text{mg L}^{-1}$ . Freeze and Cherry (1979) classify water into fresh (TDS  $<1,000 \text{ mg L}^{-1}$ ), brackish ( $>1,000 \text{ mg L}^{-1}$ ), saline ( $>10,000 \text{ mg L}^{-1}$ ) and brine ( $100,000 \text{ mg L}^{-1}$ ) categories on the basis of TDS concentration. Based on this classification, 91 % of the groundwater of the study area belongs to fresh water and remaining 9 % to brackish water categories. The higher standard deviations for the EC ( $\pm 552$ ) and TDS ( $\pm 353$ ) values reflect wide spatial variability in the ionic concentrations in the groundwater of the study area. The concentration contour of TDS shows higher values at sites 1, 4, 8, 11, 24, 54 and 63 (Fig. 2a). The large spatial differences between the values of TDS and ionic concentrations could be attributed to the variation in the lithology and anthropogenic activities in the region.

The anion chemistry shows that  $\text{HCO}_3^-$  and  $\text{Cl}^-$  are the dominant anions followed by  $\text{SO}_4^{2-}$  and  $\text{NO}_3^-$  in the abundance order of  $\text{HCO}_3^- > \text{Cl}^- > \text{SO}_4^{2-} > \text{NO}_3^- > \text{F}^-$  (Table 1). The measured concentration of  $\text{HCO}_3^-$  in the groundwater samples varies from 105 to 925  $\text{mg L}^{-1}$  with an average value of 388  $\text{mg L}^{-1}$  and it accounts for 75 % of the total anions ( $\text{TZ}^-$ ) in equivalent unit. Weathering of carbonate and/or alumino-silicate rocks with a secondary contribution from dissolution of  $\text{CO}_2$  gases are the primary source of  $\text{HCO}_3^-$  in the groundwater. The soil zone in the subsurface environment contains elevated  $\text{CO}_2$  pressure (produced as result of anoxic biodegradation of organic matter and root respiration), which in turn combines with rainwater to form bicarbonate. The higher proportions of bicarbonate in relation to other anions indicate weathering of primary silicate minerals dominated by alkaline earths (Rose 2002).

**Table 1** Hydrogeochemical characteristics of groundwater of Jhansi district

SS	Site name	Type	pH	EC	TDS	Turb	F <sup>-</sup>	Cl <sup>-</sup>	HCO <sub>3</sub> <sup>-</sup>	SO <sub>4</sub> <sup>2-</sup>	NO <sub>3</sub> <sup>-</sup>	Silica
1	Gursarai	H/P	8.0	1,969	1,586	4.9	0.9	313.9	618	84.2	131.9	24.7
2	Haibat Pur	H/P	6.8	1,180	835	1.3	2.7	132.5	403	50.1	10.2	35.9
3	Khiria	W/W	7.6	908	699	0.4	3.0	82.0	358	53.2	5.7	33.6
4	Pipra Bazar	H/P	7.3	1,331	1,068	0.6	2.0	179.9	444	64.4	91.2	13.6
5	Bashen	H/P	6.9	174	152	4.2	0.6	3.4	105	1.0	1.3	4.3
6	Dondia	H/P	7.5	808	779	0.9	2.9	5.5	567	1.1	1.4	8.1
7	Asta	H/P	7.3	848	741	1.4	1.5	32.8	523	11.9	3.1	18.4
8	Mauranipur	H/P	7.6	676	542	1.3	1.7	22.0	376	2.3	14.7	18.8
9	Kuracha Gaon	H/P	7.8	874	808	0.7	3.4	11.9	521	4.6	48.6	23.8
10	Rauni	W/W	6.8	750	586	0.4	0.1	44.7	325	33.6	30.6	33.9
11	Churara	H/P	7.1	1,585	1,268	3.1	1.2	203.9	482	113.1	129.1	26.4
12	Mathupura	W/W	7.8	593	462	1.2	2.1	9.6	312	3.4	23.2	12.4
13	Dhakarwara	W/W	7.6	685	585	0.3	1.8	10.0	376	9.4	38.9	19.4
14	Usan	H/P	7.7	388	312	10.7	3.0	9.0	211	0.6	10.8	12.6
15	Bangara	H/P	7.2	906	708	6.2	1.5	62.8	328	36.8	87.9	33.8
16	Shevara	W/W	7.4	814	573	0.8	0.8	58.0	191	27.6	129.1	41.4
17	Patha Karka	H/P	7.8	922	864	1.2	1.0	18.0	611	4.9	19.1	18.1
18	Uldan	H/P	7.5	1,066	919	4.0	2.3	76.9	510	103.5	6.9	13.1
19	Bagroni Jaageer	W/W	7.7	624	530	0.9	1.4	38.0	319	12.9	20.9	8.5
20	Gharoi	H/P	7.2	583	423	13.5	1.0	10.0	225	10.1	43.8	40.9
21	Palra	W/W	7.3	386	317	1.5	0.4	12.0	210	1.6	1.3	16.6
22	Sekra	H/P	7.1	361	277	7.3	1.4	8.0	187	5.2	9.2	11.1
23	Dakhneshwar	H/P	7.6	1,617	1,177	0.6	3.4	181.9	549	95.0	19.5	12.9
24	Dudi	H/P	8.2	803	752	1.6	3.0	20.0	486	22.6	6.6	14.8
25	Singar	H/P	7.3	677	581	1.9	1.2	43.8	356	20.6	7.6	10.7
26	Khareni	W/W	7.5	775	687	0.2	0.9	40.4	468	5.7	3.1	27.2
27	Iskil-Bujurg	H/P	7.4	747	678	0.8	0.7	20.0	479	2.6	2.0	23.2
28	Jhabra	H/P	7.4	966	890	0.6	1.7	14.0	630	2.7	2.5	23.6
29	Erichghat	H/P	7.2	1,337	971	3.1	1.0	88.0	535	56.6	19.5	24.0
30	Saria	H/P	7.4	776	626	0.8	2.2	18.0	412	3.2	1.6	26.8
31	Poonch	H/P	7.6	664	594	0.4	1.1	18.0	423	1.7	0.6	20.1
32	Sikandra	H/P	7.5	643	562	0.5	1.2	6.0	412	2.2	3.4	19.7
33	Chatgowan	H/P	7.8	835	737	2.4	3.1	14.0	512	3.2	0.7	15.6
34	Dhorka	H/P	7.6	843	728	1.3	2.3	73.0	382	87.9	5.2	18.2
35	Babai	H/P	7.6	552	458	0.3	0.9	14.0	323	3.0	0.3	11.4
36	Sesa	W/W	7.9	717	647	2.4	0.7	20.0	467	11.1	3.7	14.1
37	Kishanpura	H/P	7.3	813	693	2.3	1.0	62.0	436	19.7	4.4	12.8
38	Jhansi city	H/P	7.5	626	511	1.2	1.3	42.0	303	27.5	7.1	20.6
39	Ellite Chawraha	H/P	7.7	385	276	0.5	1.0	12.4	152	28.7	2.3	22.6
40	Jhansi Station	H/P	7.7	275	232	3.4	0.4	12.0	132	30.4	0.1	4.4
41	Sipri Bazar	H/P	7.2	825	656	6.6	0.9	68.0	329	43.5	16.8	21.3
42	Manik Chawk	H/P	7.5	486	400	7.9	2.0	16.8	258	9.2	3.9	24.3
43	Hansarai	H/P	7.8	516	455	4.7	1.7	8.0	335	5.3	1.6	10.2
44	Bijoli	H/P	7.2	578	527	2.1	0.9	46.0	311	24.0	3.1	25.9
45	Sainyar	H/P	6.7	642	501	6.7	1.2	36.0	268	41.2	15.6	28.8
46	Baghora	H/P	6.9	1,144	746	8.1	0.5	112.0	312	54.2	19.5	59.3
47	Babina Budh	H/P	6.9	930	671	1.7	1.5	84.0	287	44.4	18.8	42.6
48	Ganeshpura	H/P	7.4	698	485	1.7	1.5	44.0	226	31.6	18.3	36.3

**Table 1** continued

SS	Site name	Type	pH	EC	TDS	Turb	F <sup>-</sup>	Cl <sup>-</sup>	HCO <sub>3</sub> <sup>-</sup>	SO <sub>4</sub> <sup>2-</sup>	NO <sub>3</sub> <sup>-</sup>	Silica	
49	Khajraha-Buzurg	H/P	7.4	397	292	1.9	2.0	14.0	173	8.5	2.1	32.1	
50	Barora	H/P	7.1	1,039	749	2.4	1.6	88.0	367	44.4	18.8	34.1	
51	Rajapura	H/P	7.4	599	445	2.7	1.2	24.0	253	24.7	16.7	30.9	
52	Raksha	H/P	6.9	915	565	2.6	1.4	74.0	257	43.1	18.8	43.9	
53	Moth	H/P	7.2	1,770	1,078	2.2	2.3	209.9	435	79.5	19.5	38.3	
54	Kargawan	H/P	8.1	693	552	5.3	0.9	18.9	366	16.8	4.0	43.0	
55	Chirgoan	H/P	7.5	860	655	0.8	0.6	28.0	424	13.8	1.2	13.7	
56	Amargarh	H/P	7.4	943	709	17.2	0.9	60.0	452	24.6	0.6	16.5	
57	Semari	H/P	8.6	430	378	2.6	0.3	14.0	264	6.1	1.1	1.5	
58	Nand	H/P	8.0	786	719	14.2	0.8	30.0	506	20.0	2.3	21.0	
59	Korkos	H/P	7.9	675	646	1.1	2.7	12.0	479	5.1	0.9	13.8	
60	Baral	H/P	7.5	1,019	925	1.4	1.7	50.0	626	23.3	1.1	21.4	
61	Sultanpura	H/P	7.7	1,054	963	4.2	2.0	24.0	735	4.4	13.5	20.0	
62	Pahari-Khurg	H/P	6.9	4,450	2,667	7.0	1.3	798.0	925	160.3	33.4	24.3	
63	Gulara	H/P	7.9	1,102	987	1.6	1.9	48.0	693	34.2	18.8	23.2	
64	Parichha	H/P	8.1	403	317	9.2	0.6	10.0	214	10.1	7.5	10.8	
65	Baretha	H/P	8.0	639	557	4.3	0.7	12.6	405	3.8	2.1	18.7	
66	Baragaon	H/P	7.5	519	412	4.7	1.3	12.8	267	4.3	7.5	16.9	
67	Dunara	H/P	7.7	726	450	1.9	2.1	16.0	311	5.2	0.9	20.4	
68	Goramachia	H/P	7.2	938	711	4.9	2.1	38.0	394	58.7	11.8	24.7	
69	Konchha Bhanwar	H/P	7.5	547	381	3.4	1.2	16.0	223	19.5	9.5	32.7	
	Minimum		6.7	174	152	0.20	0.1	3.4	105	0.6	0.12	1.5	
	Maximum		8.6	4,450	2,667	17.2	3.4	798	925	160.3	131.9	59.3	
	Mean		7.5	852	673	3.3	1.5	58.8	388	27.9	18.0	22.4	
	SD		0.4	552	353	3.5	0.8	106.7	154	31.7	29.5	11.0	
SS	Ca <sup>2+</sup>	Mg <sup>2+</sup>	Na <sup>+</sup>	K <sup>+</sup>	TH	TZ <sup>-</sup>	TZ <sup>+</sup>	CAI-I	CAI-II	SAR	%Na	RSC	KI
1	56.4	110.2	242.8	3.9	594	22.9	22.5	-0.20	-0.13	4.33	47.3	-1.75	0.89
2	125.5	26.4	43.2	5.5	422	11.7	10.5	0.46	0.22	0.91	19.3	-1.83	0.22
3	61.1	36.1	64.9	1.9	301	9.5	8.9	-0.24	-0.08	1.63	32.3	-0.15	0.47
4	44.0	45.5	181.3	1.8	297	15.3	13.9	-0.56	-0.28	4.58	57.2	1.34	1.33
5	18.3	4.7	11.9	1.9	65	7.2	6.1	-4.89	-0.27	0.64	30.3	0.42	0.40
6	22.9	19.0	150.2	0.9	135	9.9	9.3	-17.59	-0.66	5.62	70.8	6.59	2.42
7	44.1	56.6	34.8	15.1	343	7.8	6.6	-1.05	-0.11	0.82	21.7	1.72	0.22
8	52.8	30.4	23.0	0.5	257	18.2	16.0	-0.63	-0.06	0.62	16.5	1.03	0.19
9	24.1	17.4	152.2	1.0	132	5.9	5.4	-14.29	-0.66	5.77	71.6	5.90	2.51
10	53.2	30.9	32.3	1.6	260	7.4	6.7	-0.15	-0.03	0.87	21.8	0.13	0.27
11	166.3	36.4	104.9	4.6	565	4.1	3.7	0.19	0.09	1.92	29.3	-3.39	0.40
12	55.2	19.6	21.2	3.1	219	9.4	8.5	-2.71	-0.13	0.62	18.7	0.75	0.21
13	55.5	19.9	52.4	1.7	220	7.5	6.6	-7.24	-0.29	1.54	34.5	1.76	0.52
14	20.3	20.6	23.4	0.5	135	11.0	10.7	-3.08	-0.21	0.87	27.6	0.75	0.38
15	84.5	29.9	38.2	4.4	334	12.9	11.1	0.00	0.00	0.91	21.0	-1.30	0.25
16	86.6	16.3	22.2	0.4	283	7.0	6.7	0.40	0.11	0.57	14.7	-2.53	0.17
17	29.8	56.7	104.9	0.7	307	4.9	5.0	-8.02	-0.39	2.60	42.7	3.87	0.74
18	64.9	45.0	95.5	1.2	347	3.9	3.7	-0.93	-0.19	2.23	37.6	1.42	0.60
19	50.6	22.3	50.8	5.9	218	3.6	3.1	-1.20	-0.22	1.50	35.1	0.87	0.51
20	67.0	15.1	10.0	0.6	230	1.9	1.9	-0.59	-0.04	0.29	8.9	-0.90	0.09

**Table 1** continued

SS	Ca <sup>2+</sup>	Mg <sup>2+</sup>	Na <sup>+</sup>	K <sup>+</sup>	TH	TZ <sup>-</sup>	TZ <sup>+</sup>	CAI-I	CAI-II	SAR	%Na	RSC	KI
21	49.0	6.3	10.9	9.2	148	9.6	9.3	-1.10	-0.11	0.39	19.3	0.48	0.16
22	32.4	12.9	9.6	0.7	134	9.9	8.8	-0.92	-0.06	0.36	14.0	0.39	0.16
23	42.6	87.3	182.3	3.1	465	16.6	17.3	-0.56	-0.25	3.68	46.2	-0.30	0.85
24	9.3	11.9	176.7	1.3	72	9.3	9.2	-12.69	-0.84	9.05	84.2	6.53	5.33
25	40.5	58.7	41.3	0.8	343	7.7	8.7	-0.47	-0.09	0.97	21.0	-1.01	0.26
26	45.5	42.6	52.0	1.6	289	9.0	8.1	-1.02	-0.15	1.33	28.5	1.90	0.39
27	49.9	28.9	70.4	1.7	243	8.5	8.0	-4.51	-0.32	1.96	39.0	2.99	0.63
28	40.0	36.6	136.6	2.1	250	10.9	11.0	-14.19	-0.54	3.76	54.5	5.32	1.19
29	65.9	72.7	106.5	2.2	464	12.8	14.0	-0.89	-0.21	2.15	33.6	-0.50	0.50
30	40.4	34.6	85.4	1.9	243	7.5	8.6	-6.42	-0.48	2.38	43.6	1.89	0.76
31	31.2	32.0	65.0	1.6	209	7.5	7.1	-4.65	-0.34	1.95	40.6	2.75	0.68
32	28.8	35.6	51.1	1.8	218	7.1	6.6	-12.43	-0.31	1.50	34.2	2.39	0.51
33	24.9	38.0	124.6	1.3	219	9.0	9.8	-12.82	-0.60	3.67	55.5	4.02	1.24
34	42.6	49.3	55.3	11.9	309	10.4	8.9	-0.32	-0.08	1.37	30.5	0.09	0.39
35	45.7	18.1	34.7	6.7	189	5.8	5.5	-3.25	-0.24	1.10	30.8	1.52	0.40
36	31.4	47.3	49.4	2.4	273	8.5	7.7	-2.92	-0.21	1.30	28.8	2.20	0.39
37	92.9	33.6	28.3	2.2	370	9.4	8.7	0.26	0.06	0.64	14.8	-0.25	0.17
38	50.8	23.7	33.5	1.1	224	6.9	6.0	-0.25	-0.05	0.97	24.9	0.49	0.32
39	28.3	9.6	18.6	0.8	110	3.5	3.0	-1.37	-0.15	0.77	27.4	0.29	0.37
40	32.6	7.5	10.8	2.2	112	3.2	2.8	-0.55	-0.07	0.44	19.0	-0.08	0.21
41	93.5	15.4	65.7	2.2	297	8.5	8.8	-0.52	-0.15	1.66	32.9	-0.54	0.48
42	37.8	12.8	29.6	5.5	147	5.1	4.4	-2.01	-0.21	1.06	32.7	1.29	0.44
43	20.8	33.2	31.4	8.3	188	5.9	5.3	-5.99	-0.24	0.99	29.5	1.72	0.36
44	61.8	19.5	33.4	0.9	235	7.0	6.2	-0.14	-0.03	0.95	23.9	0.41	0.31
45	34.6	29.9	44.5	1.3	209	6.6	6.2	-0.94	-0.17	1.34	32.0	0.21	0.46
46	129.7	23.5	33.4	1.9	421	9.7	9.9	0.52	0.25	0.71	15.2	-3.29	0.17
47	135.4	14.7	42.6	0.4	399	8.4	9.8	0.21	0.08	0.93	19.0	-3.26	0.23
48	50.2	19.0	44.8	13.3	203	6.0	6.4	-0.85	-0.23	1.37	36.0	-0.36	0.48
49	21.9	8.3	30.1	0.5	89	3.5	3.1	-2.35	-0.30	1.39	42.7	1.06	0.74
50	140.9	32.1	21.0	0.9	484	9.8	10.6	0.62	0.21	0.42	8.8	-3.66	0.09
51	58.8	13.6	21.3	0.6	203	5.7	5.0	-0.39	-0.05	0.65	18.9	0.10	0.23
52	55.7	32.5	37.5	0.7	273	7.6	7.1	0.21	0.08	0.99	23.2	-1.24	0.30
53	149.7	51.9	90.6	1.1	587	15.1	15.7	0.33	0.21	1.63	25.3	-4.60	0.34
54	44.7	29.7	27.0	1.1	234	7.0	5.9	-1.25	-0.10	0.77	20.5	1.33	0.25
55	18.8	52.9	97.6	4.0	264	8.1	9.6	-4.50	-0.49	2.61	45.1	1.66	0.80
56	28.7	88.2	35.3	2.3	434	9.7	10.3	0.06	0.01	0.74	15.5	-1.27	0.18
57	3.8	8.8	77.7	1.0	46	4.9	4.3	-7.62	-0.67	5.00	78.8	3.41	3.69
58	26.1	50.6	59.9	2.2	273	9.6	8.1	-2.15	-0.21	1.58	32.8	2.83	0.48
59	22.3	38.3	70.1	1.8	213	8.5	7.4	-8.13	-0.35	2.09	42.1	3.59	0.71
60	38.4	46.9	102.0	14.6	289	12.3	10.6	-2.41	-0.32	2.61	45.4	4.49	0.77
61	17.2	33.8	189.0	2.9	182	13.1	11.9	-11.3	-0.62	6.09	69.5	8.41	2.26
62	104.4	427.8	187.7	4.8	2019	41.6	48.7	0.63	0.75	1.82	17.0	-25.2	0.20
63	20.4	75.6	120.3	2.7	361	13.8	12.5	-2.91	-0.32	2.75	42.3	4.13	0.72
64	11.8	31.4	20.0	0.7	158	4.2	4.1	-2.15	-0.16	0.69	21.9	0.34	0.28
65	40.8	26.3	43.9	3.2	210	7.1	6.2	-4.60	-0.24	1.32	32.2	2.44	0.45
66	32.0	27.9	40.3	1.9	195	5.0	5.7	-3.99	-0.31	1.26	31.6	0.49	0.45
67	32.8	22.6	37.8	1.2	175	5.8	5.2	-2.71	-0.23	1.24	32.4	1.60	0.47

**Table 1** continued

SS	Ca <sup>2+</sup>	Mg <sup>2+</sup>	Na <sup>+</sup>	K <sup>+</sup>	TH	TZ <sup>-</sup>	TZ <sup>+</sup>	CAI-I	CAI-II	SAR	%Na	RSC	KI
68	56.9	24.9	87.9	1.4	245	9.1	8.7	-2.60	-0.35	2.45	44.1	1.57	0.78
69	44.7	19.8	12.7	1.6	193	4.7	4.5	-0.31	-0.03	0.40	13.3	-0.21	0.14
	3.8	4.7	9.6	0.4	46	1.9	1.9	-17.59	-0.84	0.29	8.8	-25.2	0.09
	166.3	427.8	242.8	15.4	2019	41.6	48.7	0.63	0.75	9.05	84.2	8.41	5.33
	51.3	38.5	65.8	2.9	287	9.0	8.7	-3.05	-0.18	1.83	32.9	0.63	0.65
	34.6	51.8	53	3.3	243	5.4	6.1	4.24	0.25	1.62	16.3	4.00	0.84

*Unit:* Concentrations are in mg L<sup>-1</sup>, except EC (μS cm<sup>-1</sup>), Turbidity (NTU) CIA (meq L<sup>-1</sup>), SAR (meq L<sup>-1</sup>), RSC (meq L<sup>-1</sup>), Na (%) and pH EC electrical conductivity, TDS total dissolved solids, TH total hardness (mg L<sup>-1</sup>), TZ<sup>-</sup> total anions (meq), TZ<sup>+</sup> total cations (meq), CAI chloro-alkaline indices, SAR sodium adsorption ratio, RSC residual sodium carbonate, KI Kelley index, H/P hand pump, W/W Dugwell, SS sampling sites, Turb. turbidity

The chloride concentration in the groundwater of Jhansi district varied between 3.4 and 798 mg L<sup>-1</sup> with an average value of 58.8 mg L<sup>-1</sup>. In an equivalent unit, Cl<sup>-</sup> constitutes 14 % of the total anions (TZ<sup>-</sup>). Chloride presents in a lower concentration in common rock types as compared to other constituents of natural water. It is assumed that bulk of the chloride in water is primarily either from atmospheric source or from seawater. Weathering of halite and evaporites is considered as the major lithogenic source of chloride. The dissolution of halite releases equal concentration of Na<sup>+</sup> and Cl<sup>-</sup> into the solution and resulting Na<sup>+</sup>/Cl<sup>-</sup> molar ratio will be approximately one. The present study area is far away from seacoast and the higher Na<sup>+</sup>/Cl<sup>-</sup> ratio (avg. 4.3) in the groundwater suggest non-lithogenic and non-atmospheric source of chloride (Jalali 2007; Singh et al. 2011). The large lateral variations and high concentrations of chloride in some groundwater samples (1, 11, 54, 63) indicate local recharge from anthropogenic sources including agricultural runoff and domestic, industrial and animal wastes (Fig. 2b).

Concentration of nitrate in the analysed groundwater samples varies between 0.10 and 131.9 mg L<sup>-1</sup> (avg. 18.0 mg L<sup>-1</sup>), constituting about 3 % of the total anionic mass balance. Nitrate is an important pollutant in the environment, generally derived from atmospheric precipitation, agricultural fertilizers, human and animal excreta, biological fixation and nitrification of organic N and NH<sub>4</sub> (Appelo and Postma 1996). The concentration contour plot of NO<sub>3</sub><sup>-</sup> shows relatively higher values in subsurface water samples 1, 4, 11, 15 and 16 (Fig. 2d). This enhancement in the concentrations of NO<sub>3</sub><sup>-</sup> are attributed to anthropogenic activities involving nitrogen compounds like fertilizers or byproducts of organic compounds from agriculture, septic systems and livestock manure (Reddy et al. 2011; Vidal et al. 2000). Urea (NH<sub>2</sub>)<sub>2</sub>CO, ammonium nitrate (NH<sub>4</sub>NO<sub>3</sub>), superphosphate and livestock manure are the commonly used fertilizers in this area. Being agricultural families, every household has a good number of animals like cows,

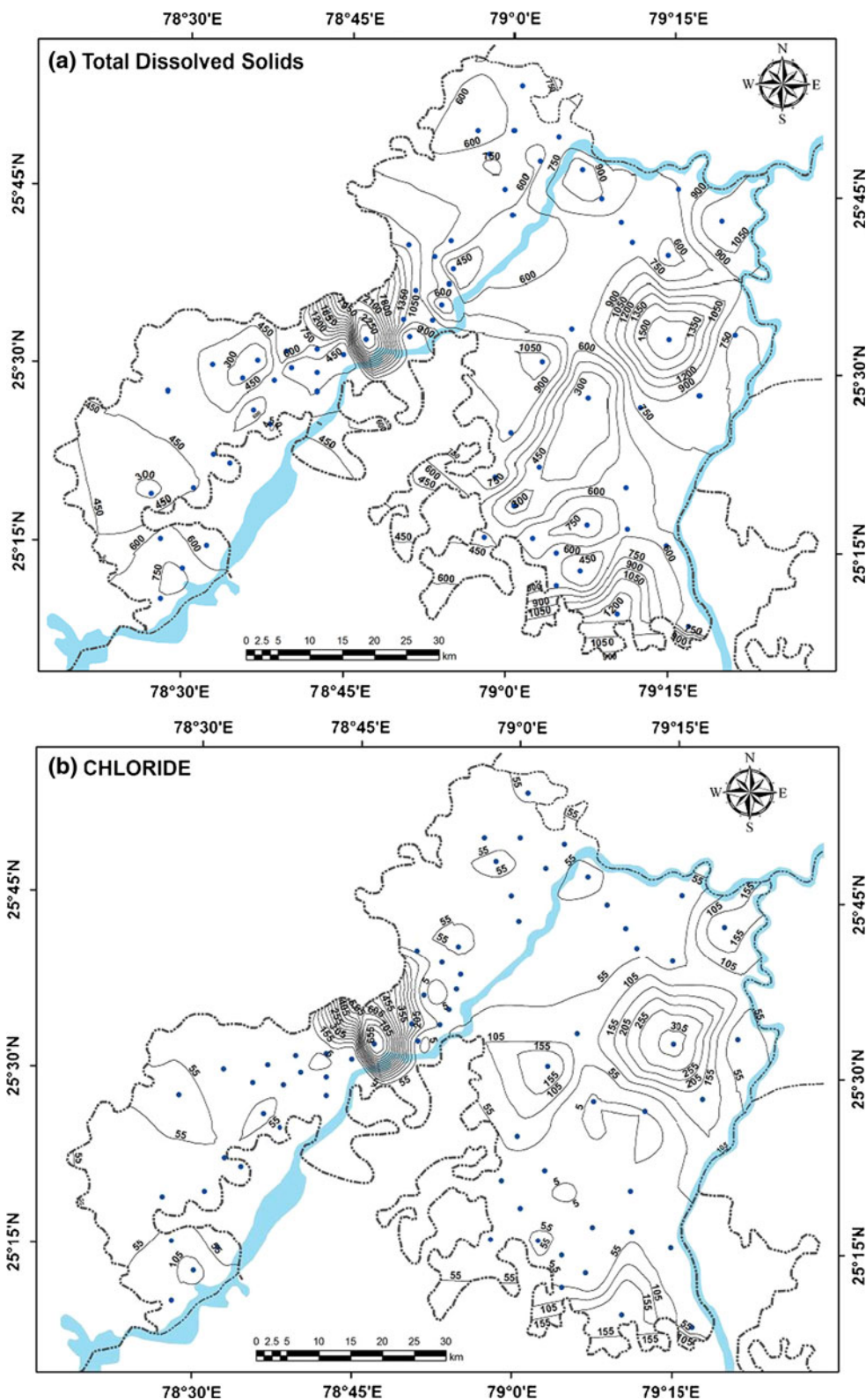
buffaloes, sheep, goats etc. for milk and agricultural activities. Most of the excreta of these domestic animals are not properly disposed and excreta, dung and urine produced by animals constitute a potential source of nitrate and chloride contamination in the groundwater. Concentration of sulphate varies from 0.6 to 160.3 mg L<sup>-1</sup> (avg. 27.9 mg L<sup>-1</sup>), contributing 6 % to the total anionic charge balance. Concentration of SO<sub>4</sub><sup>2-</sup> is relatively higher in the groundwater samples collected at sites 11, 18, 24 and 63 (Fig. 2c). Sulphate concentration in natural water is usually found between 2 and 80 mg L<sup>-1</sup> and abnormal higher concentration of sulphate may be attributed to rock weathering or anthropogenic sources like industrial and agricultural effluents (Berner and Berner 1987). A good correlation between SO<sub>4</sub><sup>2-</sup> and Cl<sup>-</sup> (0.80) and positive correlations of SO<sub>4</sub><sup>2-</sup>-NO<sub>3</sub><sup>-</sup> (0.43) and NO<sub>3</sub><sup>-</sup>-Cl<sup>-</sup> (0.38) in the groundwater of the study area support anthropogenic source of these ions (Alemayehu et al. 2010; Demlie et al. 2007).

Concentration of fluoride (F<sup>-</sup>) exceeds the drinking water desirable limits of 1.5 mg L<sup>-1</sup> in about 37 % of the groundwater samples. Fluoride concentration varied from 0.10 to 3.43 mg L<sup>-1</sup> (avg. 1.49 mg L<sup>-1</sup>) in the groundwater samples of the area and it accounts for about 1 % of the total anionic balance (Fig. 2e). Fluoride in water is mainly derived from the weathering of fluoride bearing rock forming minerals like muscovite, biotite, fluorite, fluoro-apatite etc. The higher concentration of F<sup>-</sup> in some groundwater samples may be attributed to weathering of biotite, apatite and sphene, occurred as accessories minerals in the granites and granitic gneisses of the area (Mishra and Sharma 1975).

Ca<sup>2+</sup> and Mg<sup>2+</sup> are the dominant cations in the groundwater of the Jhansi district followed by Na<sup>+</sup> and K<sup>+</sup>. On an average, alkaline earths (Ca<sup>2+</sup> + Mg<sup>2+</sup>) accounts for 67 % of the total cation concentrations (TZ<sup>+</sup>) and it dominates over the alkalis (Na<sup>+</sup> + K<sup>+</sup>). The concentration of Ca<sup>2+</sup> varies from a minimum value of 3.8 mg L<sup>-1</sup> to maximum of



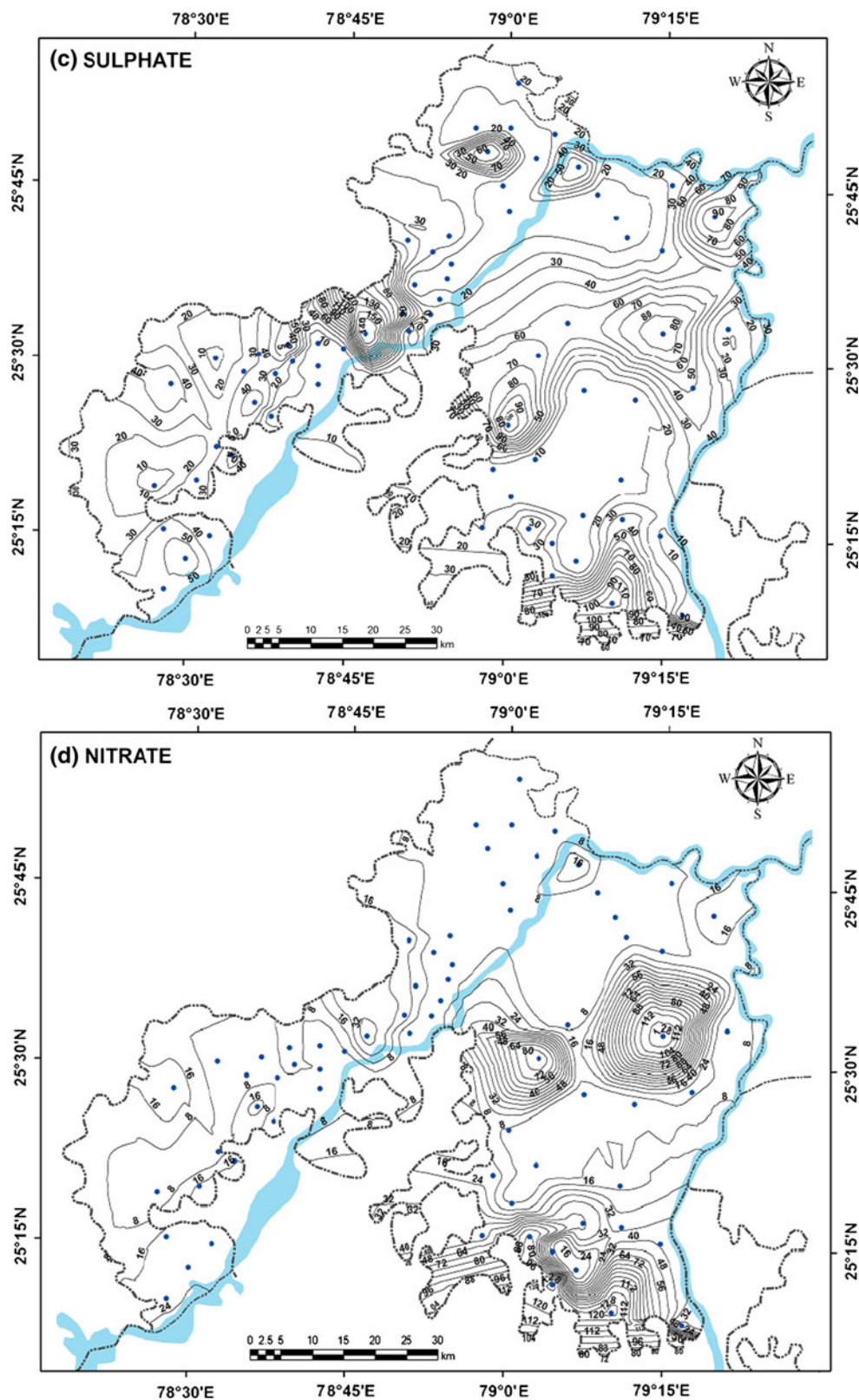
**Fig. 2** Concentration contours in  $\text{mg L}^{-1}$ , except Fe ( $\mu\text{g L}^{-1}$ ), showing spatial variations in **a** total dissolved solids, **b** chloride, **c** sulphate, **d** fluoride, **e** nitrate and **f** iron concentrations in the groundwater of Jhansi district



$166.3 \text{ mg L}^{-1}$  with an average value of  $51.3 \text{ mg L}^{-1}$  and it accounts for 34 % of the total cationic mass balance. Concentration of  $\text{Mg}^{2+}$  varies between  $4.7$  and  $427 \text{ mg L}^{-1}$

(avg.  $38.5 \text{ mg L}^{-1}$ ) and it exceeds  $\text{Ca}^{2+}$  concentration at many sites, denoting major supply from weathering of ferromagnesian minerals associated with the basic intrusive

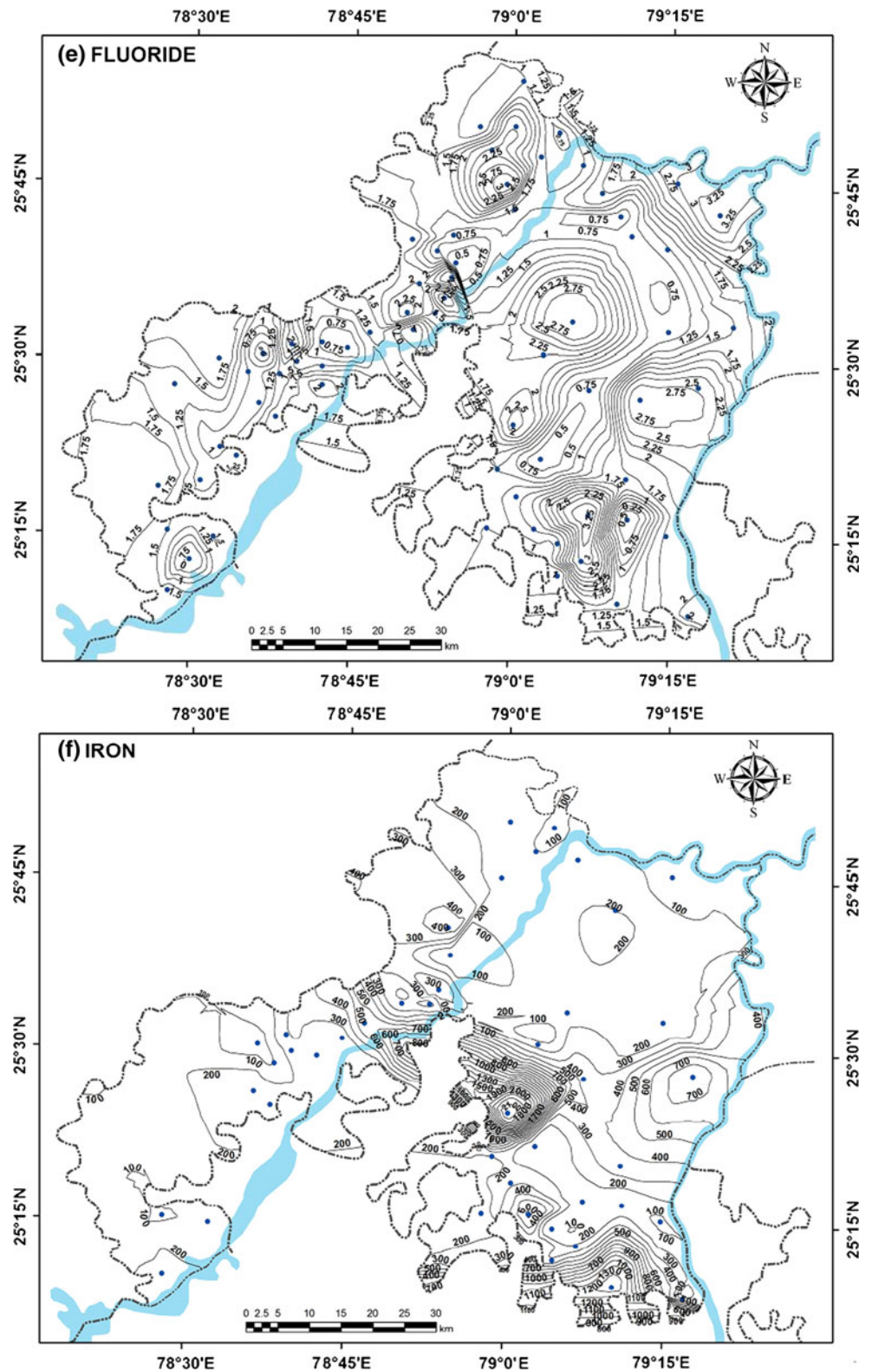
Fig. 2 continued



and ultramafic rocks of the area. Concentration of  $\text{Na}^+$  and  $\text{K}^+$  varies from 9.6 to 242.8  $\text{mg L}^{-1}$  and 0.4 to 15.1  $\text{mg L}^{-1}$ , respectively, in the groundwater of the study

area. Sodium (32 %) and potassium (1 %) are together contributing about 33 % of the total cationic charge balance. In overall cationic abundance, 45 % groundwater

Fig. 2 continued



samples are of  $\text{Ca}^{2+} > \text{Mg}^{2+} > \text{Na}^+ > \text{K}^+$ , 30 % of  $\text{Mg}^{2+} > \text{Ca}^{2+} > \text{Na}^+ > \text{K}^+$  and 23 % of  $\text{Na}^+ > \text{Mg}^{2+} > \text{Ca}^{2+} > \text{K}^+$  types.

Table 2 shows concentration of 14 trace metals analysed in 46 groundwater samples of the Jhansi district. Trace metal concentrations did not exceed the desirable limits

specified by the world health organization (WHO 2006) and Indian drinking water standards (BIS 2003) except a few exceptions. The amount of Fe ranged from 47 to 2,246  $\mu\text{g L}^{-1}$  (avg. 299  $\mu\text{g L}^{-1}$ ); exceeding the desirable limit of 300  $\mu\text{g L}^{-1}$  in about 26 % of the analysed groundwater samples (Fig. 2f). However, it exceeds the maximum permissible limit of 1,000  $\mu\text{g L}^{-1}$  in only two groundwater samples at sites 11 and 18 (BIS 2003). Iron in normal groundwater is mostly in the form of inorganic complexes derived from laterites and other types of soils. Excess Fe in groundwater is mostly accumulated through the industrial effluents discharge. However, except for agricultural based activity and stone mining and crushing, no other major anthropogenic or industrial activities has been carried out in this region. Hence, the observed higher values of Fe in the aquifer may be attributed to geogenic origin from water–rock interaction. Concentration of Mn and Zn varied between 0.9–203 and 1.6–542  $\mu\text{g L}^{-1}$  and found well within the prescribed limit for drinking uses. Concentrations of other measured toxic metals like As, Se, Pb, Cd, Cr and Co were also found to be well within the specified limit of Indian drinking water standards (BIS 2003).

### Hydrochemical classification and hydrogeochemical facies

The geochemical evolution of groundwater and relationship between different dissolved ions can be understood by plotting the geochemical data on Piper (1944) trilinear diagram. The data plot on the trilinear diagram shows that majority of groundwater samples fall into no dominant zone in the cation facies and  $\text{HCO}_3^-$  zone in the anion facies (Fig. 3). The plot of geochemical data on central diamond shaped field which relates cation and anion triangles reveals that the majority of the points fall in the zone of 1, 3, 5 and 8, indicating dominance of alkaline earth ( $\text{Ca}^{2+} + \text{Mg}^{2+}$ ) over alkalis ( $\text{Na}^+ + \text{K}^+$ ) and weak acids ( $\text{HCO}_3^-$ ) over strong acids ( $\text{SO}_4^{2-} + \text{Cl}^-$ ). Plotted points of majority of samples fall in zone 5, suggesting secondary alkalinity and carbonate hardness. About 14 % samples falls in the field 8, signifying primary alkalinity and carbonate alkali water. Trilinear diagram reveals that alkaline earths and weak acids dominate the groundwater chemistry and Ca–Mg– $\text{HCO}_3^-$  and Na– $\text{HCO}_3^-$  are the dominant hydrogeochemical facies. The rocks of the study area mainly consist of granite, granitic gneiss, dolerite, peridotites and meta-granitoids. The dominance of Ca–Mg– $\text{HCO}_3^-$  and Ca–Na– $\text{HCO}_3^-$  type water suggest water–rock interaction involving the dissolution of plagioclase feldspar, ferromagnesian minerals and carbonates by the recharging groundwater, which might evolve to Ca–Na– $\text{HCO}_3^-$  water type due to cation exchange process.

### Water–rock interaction and solute acquisition processes

The chemical composition of groundwater are controlled by a number of factors including composition of infiltrating rainwater, geological structure and mineralogical composition of country rocks and anthropogenic activities in the area (Andre et al. 2005; Datta and Tyagi 1996; Singh et al. 2008). The contribution of atmospheric sources to the dissolved salts in the water can be assessed by considering the local rainwater chemistry or by taking the ratios of elements to  $\text{Cl}^-$  (Sarin et al. 1989; Singh et al. 2005; Zhang et al. 1995). The average  $\text{Na}^+/\text{Cl}^-$  and  $\text{K}^+/\text{Cl}^-$  ratios for the subsurface water (4.36 and 0.12) in the present study area are found to be higher as compared with marine aerosols ( $\text{Na}^+/\text{Cl}^- = 0.85$  and  $\text{K}^+/\text{Cl}^- = 0.0176$ ). This suggests a limited contribution from atmospheric precipitation and reveals that high levels of major ions in the groundwater are sustained most likely by weathering of rock forming minerals. The plot of geochemical data on Gibbs's diagram (Gibbs 1970) that represent the ratio of  $\text{Na}^+ + \text{K}^+ / (\text{Na}^+ + \text{K}^+ + \text{Ca}^{2+})$  and  $\text{Cl}^- + \text{NO}_3^- / (\text{Cl}^- + \text{NO}_3^- + \text{HCO}_3^-)$  as a function of TDS also indicate dominance of rock weathering in controlling the groundwater chemistry of the study area (Fig. 4a, b). Further, high concentration of  $\text{HCO}_3^-$  and higher ratio of  $\text{HCO}_3^- / (\text{SO}_4^{2-} + \text{Cl}^-)$  i.e. 7.8 are also suggesting rock weathering as a major source with limited input from atmospheric and anthropogenic sources (Hounslow 1995; Rose 2002).

Weathering of carbonate, silicate and sulphide minerals and dissolution of evaporites are the major lithogenic source of the dissolved ions in the water. The plot of  $(\text{Ca}^{2+} + \text{Mg}^{2+})$  versus  $(\text{HCO}_3^- + \text{SO}_4^{2-})$  will be close to 1:1 line; if the dissolution of calcite, dolomite and gypsum are the dominant reactions in a system (Cerling et al. 1989; Fisher and Mullican 1997). The plotted points of the majority of the groundwater samples on the variation diagram relating  $(\text{Ca}^{2+} + \text{Mg}^{2+})$  and  $(\text{HCO}_3^- + \text{SO}_4^{2-})$  falls below the equiline, though some points approach the theoretical 1:1 trend at lower concentration (Fig. 5a). The excess of  $(\text{HCO}_3^- + \text{SO}_4^{2-})$  over  $(\text{Ca}^{2+} + \text{Mg}^{2+})$  suggests significant contribution from non-carbonate source and demanding the required portion of the  $(\text{HCO}_3^- + \text{SO}_4^{2-})$  to be balanced by the alkalis ( $\text{Na}^+ + \text{K}^+$ ). The plotted points of about 19 % samples fall above the 1:1 line indicating some extra source of cations, which should be balanced by  $\text{Cl}^-$ , the only other major anion present in the groundwater. The stoichiometry of carbonate weathering reactions demands that carbonate derived  $(\text{Ca}^{2+} + \text{Mg}^{2+})$  should be equal to the carbonate-derived  $\text{HCO}_3^-$ . The plot of  $(\text{Ca}^{2+} + \text{Mg}^{2+})$  versus  $\text{HCO}_3^-$  shows a deficiency of  $\text{Ca}^{2+} + \text{Mg}^{2+}$  relative to  $\text{HCO}_3^-$  in majority of the samples and demands that excess negative charge of

**Table 2** Concentration of trace metals in the groundwater of the Jhansi district

Sam. Site	Al	As	Ba	Bi	Cd	Co	Cu	Cr	Fe	Li	Mn	Ni	Pb	Se	Zn
1	44.5	3.2	6.3	0.33	0.03	0.11	2.9	0.42	119	0.79	24.2	0.73	4.22	0.21	15.2
2	9.0	2.5	38.8	0.04	0.03	0.19	2.8	0.60	742	5.67	40.7	1.64	3.39	0.49	123.2
3	8.0	3.7	27.0	0.09	0.06	0.12	2.0	0.80	179	18.62	67.8	1.22	3.52	0.60	5.1
4	3.9	2.7	7.1	0.03	0.02	0.08	4.1	0.83	150	6.44	1.7	0.75	3.94	0.54	8.2
5	5.9	0.8	4.5	1.60	0.09	0.14	11.9	BDL	373	0.14	17.1	0.81	5.84	0.12	242.6
8	17.2	2.9	16.9	0.03	0.05	0.10	5.5	1.53	344	3.03	5.5	1.06	5.64	0.37	105
9	15.1	2.3	7.8	0.03	0.02	0.06	1.8	0.92	152	7.26	5.5	0.49	4.28	0.09	6.3
10	13.0	2.8	7.1	0.08	0.03	0.09	3.0	0.94	150	6.96	1.0	1.12	7.09	0.52	17.2
11	32.5	9.2	163.7	0.08	0.15	0.38	11.6	1.53	1,345	5.27	8.8	4.70	13.11	4.92	29.9
12	5.6	2.1	24.0	0.01	0.05	0.05	3.0	0.40	191	2.38	3.2	0.61	5.57	0.55	49.6
13	10.4	3.1	27.2	0.02	0.05	0.01	1.3	1.01	91	6.39	1.2	0.68	3.53	0.44	2.5
14	35.7	3.6	6.1	0.01	0.03	0.10	3.2	1.25	227	1.93	6.5	0.62	5.04	0.47	51.8
15	12.3	2.5	17.4	0.01	0.03	0.10	4.2	0.46	604	2.92	4.9	1.08	4.35	0.48	7.6
16	12.9	3.0	36.5	0.02	0.05	0.09	2.6	0.61	343	1.64	1.8	1.19	4.94	0.55	54.5
17	5.2	2.4	25.2	0.02	0.04	0.07	1.4	0.59	205	4.99	2.9	0.70	3.57	0.52	17.0
18	5.1	2.8	36.5	0.02	0.04	0.17	7.8	1.20	2,246	5.13	9.1	1.40	4.28	0.46	52.8
19	BDL	11.3	18.0	BDL	BDL	0.06	0.2	BDL	109	3.15	5.6	1.10	BDL	BDL	1.6
20	15.6	11.6	38.7	BDL	BDL	0.06	17.7	BDL	113	1.62	9.2	1.23	BDL	BDL	BDL
21	12.3	11.4	18.0	BDL	BDL	0.08	0.1	BDL	130	0.21	56.7	0.58	BDL	BDL	26.1
22	15.9	11.4	4.7	BDL	BDL	0.06	0.6	BDL	286	1.25	76.1	0.39	BDL	BDL	21.2
24	5.4	2.1	4.6	0.13	0.09	0.03	3.1	BDL	63	6.63	1.6	0.47	4.91	0.36	39.3
27	5.6	1.5	11.8	0.05	0.05	0.07	5.0	1.38	200	2.68	2.2	0.75	5.45	0.24	77.0
29	2.9	1.1	11.1	0.02	0.04	0.06	2.9	1.32	148	3.36	1.5	0.71	9.23	0.67	20.4
30	2.9	1.1	11.1	0.02	0.04	0.06	2.0	1.32	148	3.36	1.5	0.71	9.23	0.67	20.4
31	2.4	1.0	13.3	0.02	0.03	0.04	0.3	BDL	102	2.49	1.4	0.52	4.46	0.16	4.2
33	64.6	1.8	9.1	0.02	0.09	0.15	1.8	BDL	167	3.97	15.1	0.85	4.75	0.32	36.2
36	25.6	2.5	18.8	0.07	0.15	0.11	3.9	BDL	86	4.11	3.7	0.97	5.62	0.43	19.9
38	1.4	1.5	9.2	0.01	0.08	0.06	2.9	BDL	104	1.67	0.9	0.55	4.07	0.15	6.6
40	94.8	2.3	7.6	0.02	0.10	0.05	4.6	BDL	78	0.55	3.9	0.70	4.55	0.14	3.5
41	4.4	1.8	21.3	0.01	0.09	0.08	4.0	BDL	278	2.69	4.1	0.94	3.71	0.23	6.7
43	2.7	0.3	12.4	0.01	0.05	0.09	5.1	BDL	250	0.95	33.7	0.69	3.37	BDL	9.3
44	2.9	0.4	17.8	0.02	0.06	0.08	3.9	BDL	402	0.76	7.1	1.00	4.94	BDL	25.0
45	3.5	0.2	20.9	0.01	0.06	0.07	1.7	BDL	254	2.05	38.8	1.00	2.77	0.14	6.6
47	2.0	0.2	10.9	0.01	0.06	0.03	2.4	BDL	95	1.60	1.7	0.50	2.82	0.31	4.4
48	3.1	0.1	4.4	0.01	0.11	0.03	2.9	BDL	109	1.45	163.5	0.42	7.17	0.00	221.8
53	7.0	0.8	26.5	0.01	0.17	0.06	3.6	BDL	129	4.82	6.3	0.96	3.90	0.15	14.5
54	55.7	0.1	13.5	0.00	0.20	0.11	2.7	BDL	349	2.37	6.8	0.74	8.88	0.05	120.6
56	12.1	0.2	20.9	0.00	0.09	0.07	0.1	BDL	413	3.42	10.3	0.57	3.10	0.24	35.1
57	12.4	7.5	2.9	0.01	0.12	0.03	2.1	0.76	47	2.65	2.7	0.37	3.17	0.05	46.5
60	5.7	0.2	10.8	0.00	0.20	0.04	2.4	BDL	93	3.34	2.6	0.58	3.47	0.33	6.9
62	58.7	2.5	383.3	0.02	0.07	0.47	10.8	0.49	543	29.76	28.4	4.63	5.53	17.54	23.6
64	98.4	0.4	15.5	0.01	0.05	0.22	3.7	BDL	254	8.71	7.4	1.34	4.05	0.08	33.8
66	23.4	0.2	31.6	0.01	0.05	0.22	2.8	BDL	230	4.83	29.2	0.93	2.79	0.18	89.5
68	3.1	0.1	10.8	0.02	0.23	0.08	9.2	BDL	286	4.85	7.1	1.60	6.13	0.71	541.5
69	1.8	0.1	7.8	0.00	0.04	0.04	4.6	BDL	243	1.70	1.6	0.65	3.52	0.17	26.0

Units: Concentration in  $\mu\text{g L}^{-1}$ , *BDL* below detection limit

**Fig. 3** Piper trilinear diagram showing hydrogeochemical character of groundwater and hydrochemical facies

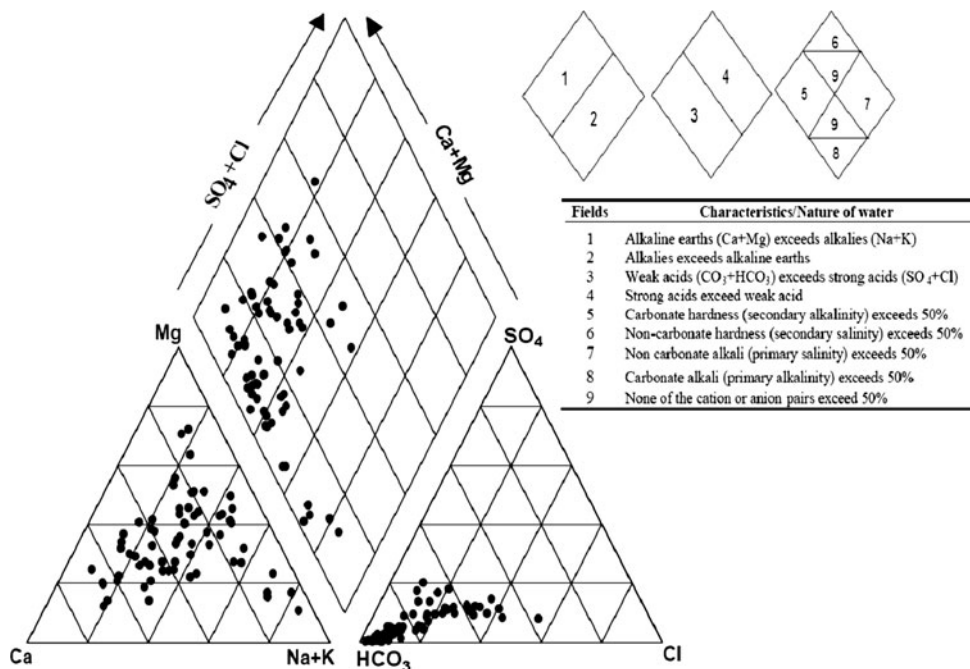
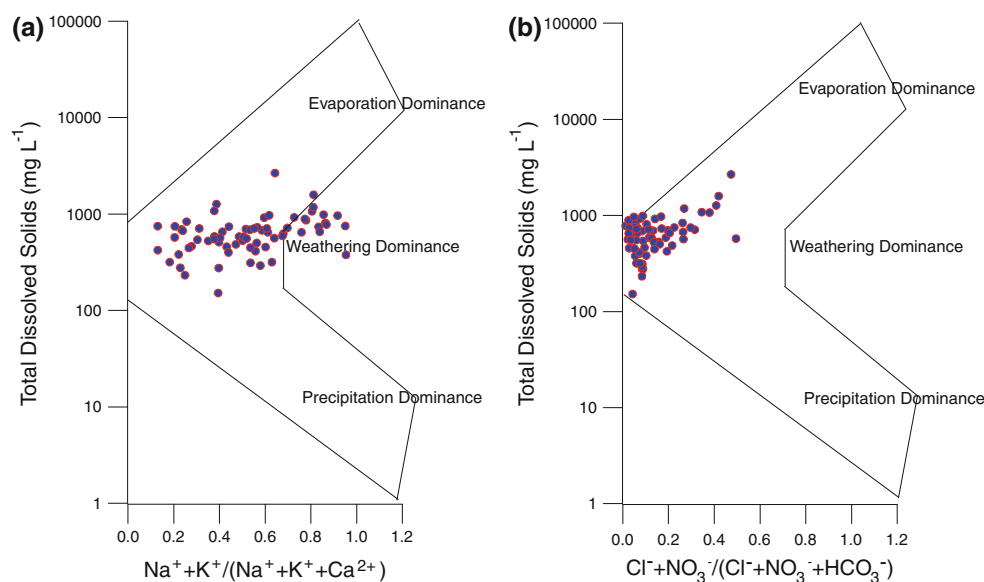


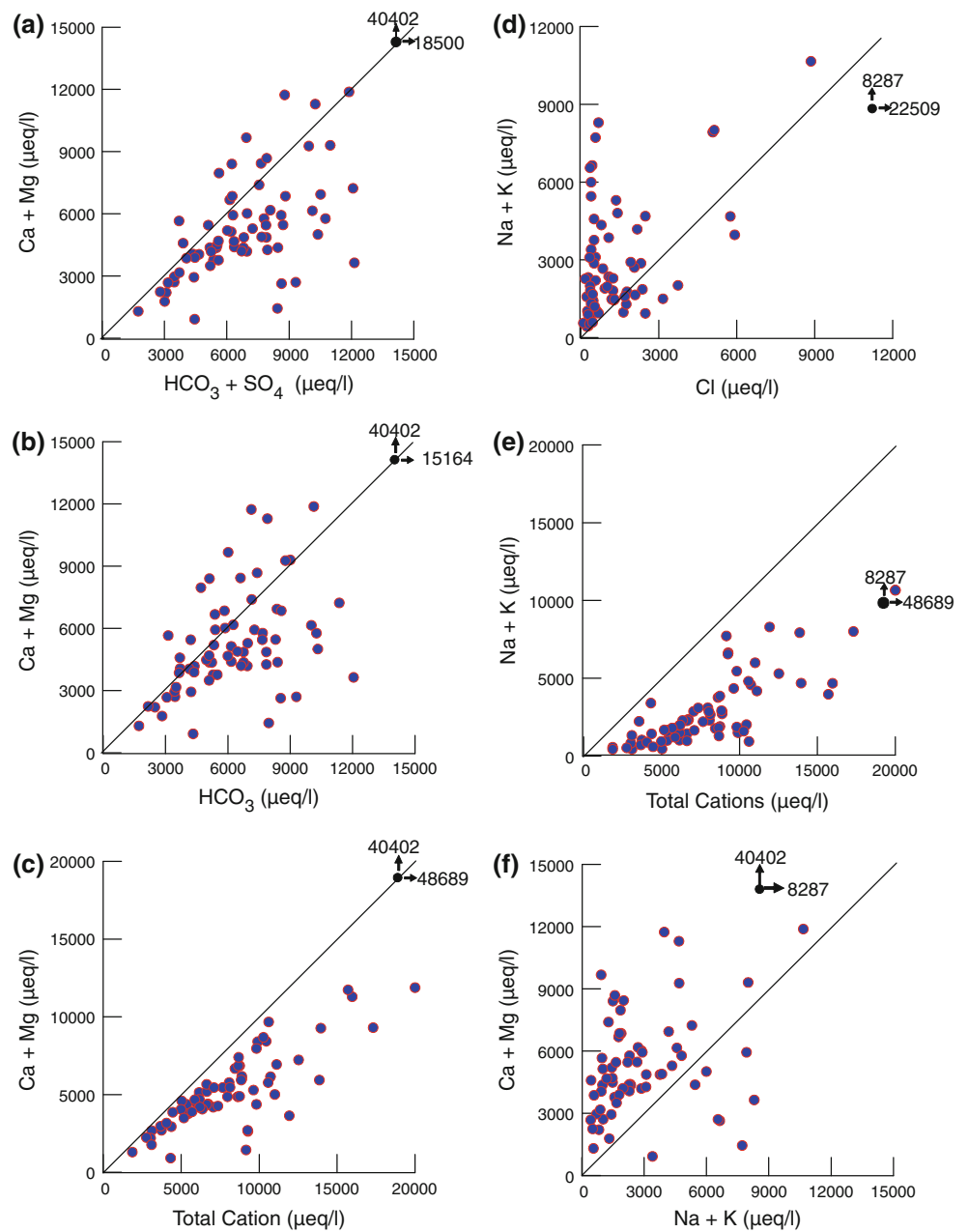
**Fig. 4** Gibbs's diagram representing the ratio of **a**  $\text{Na}^+ + \text{K}^+$  /  $(\text{Na}^+ + \text{K}^+ + \text{Ca}^{2+})$  and **b**  $\text{Cl}^- + \text{NO}_3^-$  /  $(\text{Cl}^- + \text{NO}_3^- + \text{HCO}_3^-)$  as a function of TDS



bicarbonate alkalinity should be balanced by the alkalies ( $\text{Na}^+ + \text{K}^+$ ) provided through silicate weathering. In some samples, ( $\text{Ca}^{2+} + \text{Mg}^{2+}$ ) content is slightly in excess of  $\text{HCO}_3^-$  suggesting that excess ( $\text{Ca}^{2+} + \text{Mg}^{2+}$ ) in these water should be balanced by  $\text{SO}_4^{2-}$  and  $\text{Cl}^-$  (Fig. 5b). The poor correlations between  $\text{Ca}^{2+}$ – $\text{HCO}_3^-$  (0.043) and  $\text{Ca}^{2+}$ – $\text{SO}_4^{2-}$  (0.48) indicate that calcite and gypsum dissolution are not the major contributor for the dissolved ions in the present case (Table 3). The low correlation of  $\text{Ca}^{2+}$  with  $\text{HCO}_3^-$  may indicate that large fractions of  $\text{Ca}^{2+}$  derived from other sources including anthropogenic inputs.

The plot of ( $\text{Ca}^{2+} + \text{Mg}^{2+}$ ) versus total cations ( $\text{TZ}^+$ ) shows that the plotted points fall below the equiline and the departure from 1:1 line being more pronounced at higher concentration, reflecting an increasing contribution of  $\text{Na}^+$  and  $\text{K}^+$  with increasing dissolved solids (Fig. 5c). The sodium and potassium in water are mainly derived from the atmospheric sources and/or from the weathering of alkaline silicates rich in Na and K. The concentrations of ( $\text{Na}^+ + \text{K}^+$ ) in the analysed water samples are significantly in excess over chloride and high ( $\text{Na}^+ + \text{K}^+$ )/ $\text{Cl}^-$  ratio i.e. 4.46, suggesting that much of the alkalies originate from the source other than precipitations and probably from the

**Fig. 5** Scatter plot between **a** Ca + Mg versus HCO<sub>3</sub> + SO<sub>4</sub>, **b** Ca + Mg versus HCO<sub>3</sub>, **c** Ca + Mg versus total cations, **d** Na + K versus Cl, **e** Na + K versus total cations and **f** Ca + Mg versus Na + K. Symbol  $\uparrow$  represent the plotted point projection of sample No. 62



weathering of Na and K silicates (Fig. 5d). Na<sup>+</sup> and K<sup>+</sup> are together contributing 33 % of the total cationic balance (TZ<sup>+</sup>); high (Na<sup>+</sup> + K<sup>+</sup>)/TZ<sup>+</sup> i.e. 0.33; and low (Ca<sup>2+</sup> + Mg<sup>2+</sup>)/(Na<sup>+</sup> + K<sup>+</sup>) i.e. 2.8 ratios suggest that the chemical composition of the water is largely controlled by silicate weathering reactions with limited contribution via carbonate dissolution (Fig. 5e, f).

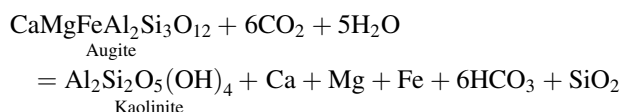
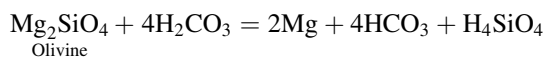
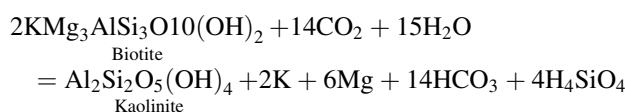
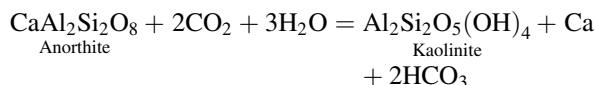
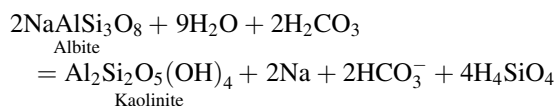
The water composition derived from the dissolution of carbonate lithology are characterized by higher calcium and magnesium concentrations and have high ratios of Ca<sup>2+</sup>/Na<sup>+</sup> i.e. 50, Mg<sup>2+</sup>/Na<sup>+</sup> i.e. 10, HCO<sub>3</sub><sup>-</sup>/Na<sup>+</sup> i.e. 120 (Gaillardet et al. 1999). The molar Ca<sup>2+</sup>/Na<sup>+</sup> ratio of average continental crust is close to 0.6 (Taylor and

MacLennan 1985), and due to the higher solubility of Na<sup>+</sup> relative to Ca<sup>2+</sup>, lower Ca<sup>2+</sup>/Na<sup>+</sup> molar ratio are expected in the dissolved loads of water draining silicate terrains. The chemical composition assigned for the silicate end member is Ca<sup>2+</sup>/Na<sup>+</sup> = 0.35 ± 0.15, Mg<sup>2+</sup>/Na<sup>+</sup> = 0.24 ± 0.12, HCO<sub>3</sub><sup>-</sup>/Na<sup>+</sup> = 2 ± 1 (Gaillardet et al. 1999). The geochemical data plotted on bivariate plot of HCO<sub>3</sub><sup>-</sup>/Na<sup>+</sup> versus Ca<sup>2+</sup>/Na<sup>+</sup> and Ca<sup>2+</sup>/Na<sup>+</sup> versus Mg<sup>2+</sup>/Na<sup>+</sup> relating carbonate and silicate end members depict the influence of silicate weathering in solute acquisition processes (Fig. 6). Thus, the hydrogeochemical data of the Jhansi district suggests weathering of aluminosilicates and ferromagnesian minerals like plagioclase feldspar, mica, amphiboles

**Table 3** Inter-elemental correlation matrix of dissolved ions ( $n = 69$ )

	pH	EC	TDS	F <sup>-</sup>	Cl <sup>-</sup>	HCO <sub>3</sub> <sup>-</sup>	SO <sub>4</sub> <sup>2-</sup>	NO <sub>3</sub> <sup>-</sup>	Silica	Ca <sup>2+</sup>	Mg <sup>2+</sup>	Na <sup>+</sup>	K <sup>+</sup>
pH	1.000												
EC	-0.244	1.000											
TDS	-0.138	0.961	1.000										
F <sup>-</sup>	0.091	0.149	0.198	1.000									
Cl <sup>-</sup>	-0.277	0.950	0.875	0.036	1.000								
HCO <sub>3</sub> <sup>-</sup>	0.113	0.695	0.835	0.281	0.500	1.000							
SO <sub>4</sub> <sup>2-</sup>	-0.339	0.788	0.734	0.125	0.807	0.349	1.000						
NO <sub>3</sub> <sup>-</sup>	-0.137	0.357	0.393	-0.045	0.381	0.096	0.424	1.000					
Silica	-0.466	0.204	0.124	-0.061	0.170	-0.086	0.255	0.275	1.000				
Ca <sup>2+</sup>	-0.579	0.452	0.375	-0.052	0.466	0.043	0.479	0.413	0.582	1.000			
Mg <sup>2+</sup>	-0.135	0.893	0.839	0.006	0.896	0.630	0.611	0.139	-0.004	0.168	1.000		
Na <sup>+</sup>	0.195	0.621	0.754	0.411	0.482	0.786	0.411	0.319	-0.144	-0.065	0.454	1.000	
K <sup>+</sup>	-0.036	0.092	0.127	0.008	0.095	0.152	0.108	-0.043	-0.085	0.002	0.121	0.011	1.000
TH	-0.325	0.944	0.869	-0.014	0.951	0.568	0.742	0.269	0.204	0.504	0.936	0.374	0.107

and pyroxenes as the major lithogenic contributor for Na<sup>+</sup>, K<sup>+</sup>, Ca<sup>2+</sup>, Mg<sup>2+</sup>, HCO<sub>3</sub><sup>-</sup> and SiO<sub>2</sub> along with minor addition of Ca<sup>2+</sup>, Mg<sup>2+</sup> and HCO<sub>3</sub><sup>-</sup> from dissolution of carbonates. The regional geology of the district also favors silicate weathering as a probable source for cations and bicarbonate. A general reaction for the weathering of silicate rocks with carbonic acid can be written as:



### Chloro-alkaline indices (CAI)

The ion exchange between the groundwater and its host environment during residence or in movement processes are the important controlling factors for water chemistry of the region. The ion exchange process can be understood by chloro-alkaline indices, also known as Schoeller index (Schoeller 1977) and expressed as:

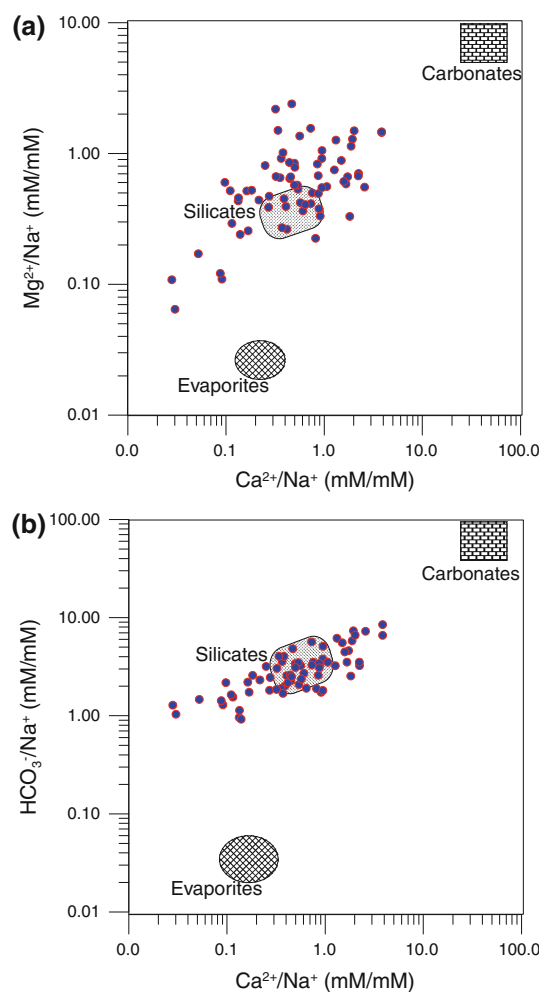


**Fig. 6** Scatter plot of **a** Mg<sup>2+</sup>/Na<sup>+</sup> versus Ca<sup>2+</sup>/Na<sup>+</sup> and **b** HCO<sub>3</sub><sup>-</sup>/Na<sup>+</sup> versus Ca<sup>2+</sup>/Na<sup>+</sup> relating carbonate and silicate end members (mM)



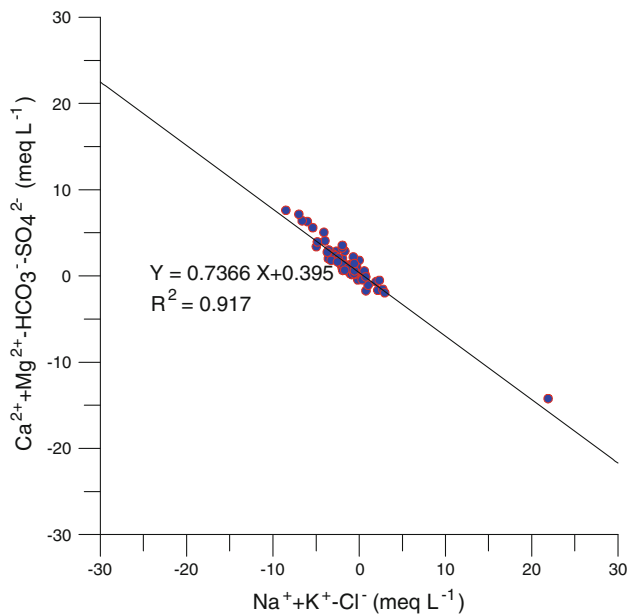


**Fig. 7** Bivariate plot between  $\text{Ca}^{2+} + \text{Mg}^{2+} - \text{HCO}_3^- - \text{SO}_4^{2-}$  versus  $\text{Na}^+ + \text{K}^+ - \text{Cl}^-$

$$\text{CAI} - \text{I} = \frac{\text{Cl}^- - (\text{Na}^+ + \text{K}^+)}{\text{Cl}^-}$$

$$\text{CAI} - \text{II} = \frac{\text{Cl}^- (\text{Na}^+ + \text{K}^+)}{\text{SO}_4^{2-} + \text{HCO}_3^- + \text{NO}_3^-}$$

The chloro-alkaline indices (CAI-I and CAI-II) can be either positive or negative depending on whether exchange of  $\text{Na}^+$  and  $\text{K}^+$  is from water with  $\text{Mg}^{2+}$  and  $\text{Ca}^{2+}$  in rock/soil or vice versa. If  $\text{Na}^+$  and  $\text{K}^+$  are exchanged in water with  $\text{Mg}^{2+}$  and  $\text{Ca}^{2+}$ , the value of the ratio will be positive, indicating a base-exchange phenomenon. The negative values of the ratio will indicate chloroalkaline disequilibrium and the reaction as a cation–anion exchange reaction. During this process, the host rocks are the primary source of dissolved solids in the water. In the present case, about 83 % of the groundwater samples have negative CAI values revealing chloro-alkaline disequilibrium and the reaction as a cation–anion exchange reaction. In 17 % of the groundwater samples, the values are positive, indicating a base-exchange reaction (Table 1). Groundwater with a base-exchange reaction in which alkaline earths have been exchanged for  $\text{Na}^+$  ion ( $\text{HCO}_3^- > \text{Ca}^{2+} + \text{Mg}^{2+}$ ) may be referred as base-exchanged softened water, and those in which  $\text{Na}^+$  ions have been exchanged for the alkaline earths ( $\text{Ca}^{2+} + \text{Mg}^{2+} > \text{HCO}_3^-$ ) referred as base exchange hardened water. In the Jhansi district, 68 % of the collected samples have higher  $\text{HCO}_3^-$  than alkaline earths ( $\text{HCO}_3^- > \text{Ca}^{2+} + \text{Mg}^{2+}$ ) indicating exchange of  $\text{Na}^+$  for alkaline earths and the water as base exchange softened water.

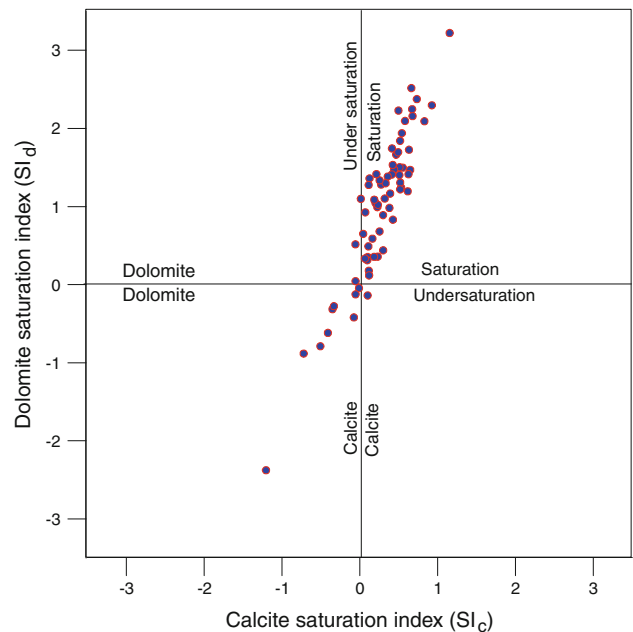


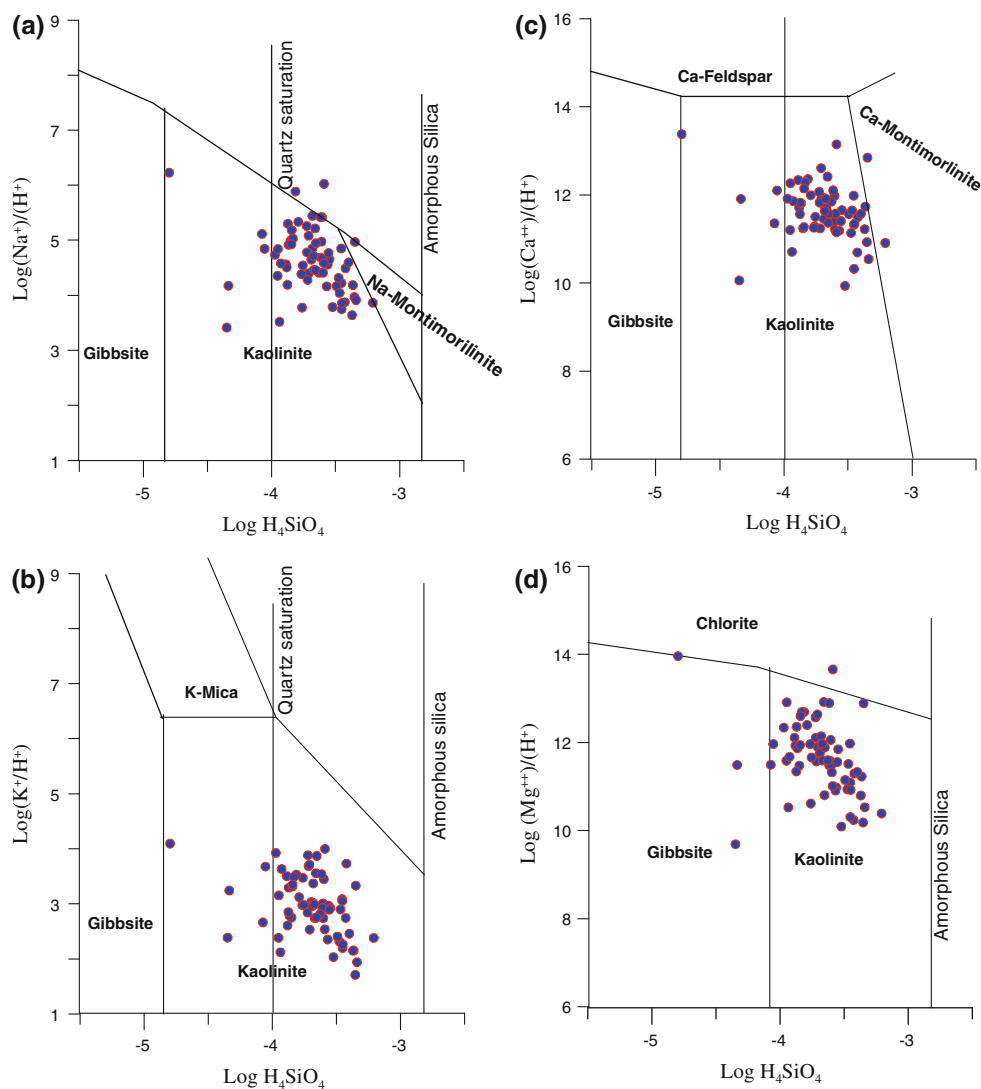
**Fig. 8** Relationship between calcite ( $\text{SI}_c$ ) and dolomite ( $\text{SI}_d$ ) saturation indices

The evidence for cation exchange can be also verified by plotting the data on bivariate plot of  $\text{Ca}^{2+} + \text{Mg}^{2+} - \text{HCO}_3^- - \text{SO}_4^{2-}$  versus  $\text{Na}^+ + \text{K}^+ - \text{Cl}^-$ .  $\text{Na}^{2+} + \text{K}^+ - \text{Cl}^-$  represents the amount of  $\text{Na}^+ + \text{K}^+$  gained or lost relative to that provided by chloride salt; while  $\text{Ca}^{2+} + \text{Mg}^{2+} - \text{HCO}_3^- - \text{SO}_4^{2-}$  represents the amount of  $\text{Ca}^{2+}$  and  $\text{Mg}^{2+}$  gained or lost relative to that provided by gypsum, calcite and dolomite dissolution. If cation exchange were an important composition controlling process, the relation between these parameters would be linear with a slope of  $-1$  (McLean et al. 2000). The bivariate plot for Jhansi groundwater indicates an increase in  $\text{Na}^+ + \text{K}^+$  related to decrease in  $\text{Ca}^{2+} + \text{Mg}^{2+}$  or an increase in  $\text{HCO}_3^- + \text{SO}_4^{2-}$ . The plotted points are close to a straight line ( $r^2 = 0.92$ ) with a slope of  $-0.71$  (Fig. 7). This indicates that almost all Na, Ca and Mg participate in the ion exchange reactions (García et al. 2001).

### Saturation indices and water mineral equilibrium

The equilibrium state of the water with respect to a mineral phase can be determined by calculating a saturation index (SI) using analytical data (Garrels and Mackenzie 1971; Stumm and Morgan 1981). By using the saturation indices (SI), it is possible to predict the reactive mineralogy of the subsurface from groundwater data without collecting the samples of the solid phase and analyzing mineralogy (Deutsch 1997). Saturation indices (SI) is defined as the

**Fig. 9** Mineral stability diagrams for silicate system



logarithm of the ratio of ion activity product (IAP) to the mineral equilibrium constant at a given temperature and express as:

$$SI = \log_{10} (IAP/K_{sp}) \quad IAP = \text{ion activity product}$$

$K_{sp}$  = solubility product at given temperature

A positive SI specifies that the water is oversaturated with respect to the particular mineral phase and therefore incapable of dissolving more of the mineral and under suitable physico-chemical condition, the mineral phase in equilibrium may precipitate. A negative indices indicates undersaturation condition and dissolution of mineral phase, while neutral SI is in equilibrium state with the mineral phase. The plot of saturation indices of calcite ( $SI_c$ ) versus dolomite ( $SI_d$ ) demonstrate that 86 % of the groundwater samples are oversaturated with respect to dolomite and calcite and the  $SI_d$  values are higher than the  $SI_c$  values (Fig. 8). The oversaturation indicates the precipitation of

calcium as Ca and/or Ca–Mg carbonate under suitable physico-chemical condition. Presence of calcareous nodules (kankar), which contain a mixture of calcite and dolomite in the sub-surface profile in the study area, suggests precipitation of Ca–Mg carbonates. About 14 % of the analysed water samples have negative SI indices and water is undersaturated with respect to both calcite and dolomite. An analysis plotting in this field represents water that has come from an environment where calcite and dolomite are depleted or where Ca and Mg exist in other forms. Water that has not reached equilibrium with the carbonates because of short residence time would also probably fall in this field. Waters of this type will dissolve calcite and/or dolomite if it encounters the source rocks.

The mineral stability is an important way in which the approach to equilibrium between clay minerals and natural water can be verified through thermodynamic data (Garrels and Christ 1965). Figure 9 shows the behavior of

**Table 4** Statistical summary of measured parameters, compared to WHO and Indian standards for drinking water

Parameters	Minimum	Maximum	Average	SD	WHO (2006)	BIS (2003) IS:10500	
						Maximum desirable	Highest permissible
<b>Major ions (mg L<sup>-1</sup>)</b>							
pH	6.7	8.6	7.5	0.4	7.0–8.5	6.5–8.5	8.5–9.2
EC (μS cm <sup>-1</sup> )	174	4,450	852	552	750	–	–
TDS	152	2,667	673	353	500	500	2,000
Turbidity (NTU)	0.2	17.2	3.3	3.5	<5.0	<5.0	–
F <sup>-</sup>	0.10	3.43	1.49	0.80	0.6–1.5	1.0	1.5
Cl <sup>-</sup>	3.4	798.0	58.8	106.7	250	250	1,000
HCO <sub>3</sub> <sup>-</sup>	105	925	388	154	200	200	600
SO <sub>4</sub> <sup>2-</sup>	0.62	160.3	27.9	31.7	200	200	400
NO <sub>3</sub> <sup>-</sup>	0.12	131.9	18.0	29.5	50	45	100
Silica	1.5	59.3	22.4	11.0	–	–	–
Ca <sup>2+</sup>	3.8	166.3	51.3	34.6	75	75	200
Mg <sup>2+</sup>	4.7	427.8	38.5	51.8	30	30	100
Na <sup>+</sup>	9.6	242.8	65.8	53.0	200	–	–
K <sup>+</sup>	0.4	15.4	2.9	3.3	–	–	–
TH	46	2,019	287	243	500	300	600
<b>Trace metals (μg L<sup>-1</sup>)</b>							
Al	1.4	98.4	19.1	24.7	100–200	–	–
As	0.1	11.6	2.9	3.3	10	50	No relaxation
Ba	2.9	383.3	28.5	59.0	300	1,000	5,000
Bi	0.00	1.60	0.08	0.05	–	–	–
Cd	0.02	0.23	0.12	0.14	3.0	10	No relaxation
Co	0.01	0.83	0.12	0.14	–	–	–
Cr	0.4	2.5	1.0	0.5	50	50	No relaxation
Cu	0.1	17.7	3.9	3.5	2,000	50	1,500
Fe	47	2,246	299	370	300	300	1,000
Mn	0.9	203.3	20.3	39.6	100	100	300
Ni	0.37	7.13	1.14	1.24	20	–	–
Pb	2.8	13.1	5.0	2.1	10	50	No relaxation
Se	0.00	17.54	0.93	2.81	10	10	No relaxation
Zn	1.6	541.5	50.8	91.0	4,000	5,000	15,000

groundwater in the silicate systems—(a) CaO–Al<sub>2</sub>–SiO<sub>2</sub>–H<sub>2</sub>O, (b) MgO–Al<sub>2</sub>–SiO<sub>2</sub>–H<sub>2</sub>O (c) Na<sub>2</sub>O–Al<sub>2</sub>–SiO<sub>2</sub>–H<sub>2</sub>O and (d) K<sub>2</sub>–Al<sub>2</sub>–SiO<sub>2</sub>–H<sub>2</sub>O at 25 °C. It demonstrates that the majority of data points fall in the range of the stability field of kaolinite. This implies that the chemistry of the water is favoring kaolinite formation. Stability in the kaolinite field suggests that infiltrating water that is enriched in soil CO<sub>2</sub> reacts with silicate minerals contained in the host rock, particularly in plagioclase feldspar and converted into allophone–hallosite–kaolinite. The infiltrating water leached out Ca, Mg, Na and HCO<sub>3</sub> from the host silicates and results a more silica rich clay minerals. Studies reported the presence of kaolinite in the lithological succession of the area (Rao et al. 2011; Jha et al. 2012).

**Water quality assessment**

The data obtained by hydrogeochemical analyses were evaluated in terms of its suitability for drinking and irrigation uses.

**Potability of groundwater for domestic uses**

The analysed parameters were compared with the standard guideline values recommended by the World Health Organisation (WHO 2006) and Bureau of Indian Standards (BIS 2003) for drinking and public health purposes (Table 4). The pH of the Jhansi groundwater samples (6.7–8.3) are well within the safe limit of 6.5–8.5, prescribed for drinking water. The turbidity is one of the

important physical parameters for water quality defining the presence of suspended solids in water and causes the muddy or turbid appearance of water body. The consumption of high turbid water may cause a health risk as excessive turbidity can protect pathogenic microorganisms from effects of disinfectants and stimulate the growth of bacteria during storage. In the study area, the turbidity ranges from 0.2 to 17.2 NTU and exceeds the recommended value of 5 NTU in 18 % groundwater samples. The values of total dissolved solids (TDS) exceed the desirable limit of 500 mg L<sup>-1</sup> in 69 % samples and maximum permissible limit of 1,000 mg L<sup>-1</sup> in 12 % groundwater samples of Jhansi district. Hardness of the water is the property attributed to the presence of alkaline earths. Water can be classified into soft (TDS <75 mg L<sup>-1</sup>), moderately hard (75–150 mg L<sup>-1</sup>), hard (150–300 mg L<sup>-1</sup>) and very hard (>300 mg L<sup>-1</sup>) based on hardness (Sawyer and McCarty 1967). The total hardness (TH) of the analysed sub-surface water of the study area varies between 46 and 2,019 mg L<sup>-1</sup> (avg. 287 mg L<sup>-1</sup>) indicating soft to very hard types of groundwater. The analytical data indicate that 27 % groundwater samples have hardness higher than 300 mg L<sup>-1</sup>, which is the desirable limit for drinking uses (Table 1). Hardness of water prevents lather formation with soap and increases the boiling point of the water. The high hardness may cause precipitation of calcium carbonate and encrustation on water supply distribution systems. The long-term consumption of extremely hard water might lead to an increased incidence of urolithiasis, anencephaly, parental mortality and cardio-vascular disorders (Agrawal and Jagetia 1997; Durvey et al. 1991). Concentration of NO<sub>3</sub><sup>-</sup> is higher than the recommended level of 45 mg L<sup>-1</sup> in 9 % of the groundwater samples. Excessive NO<sub>3</sub><sup>-</sup> in drinking water can cause a number of disorders including methaemoglobinemia in infants, gastric cancer, goiter, birth malformations and hypertension (Majumdar and Gupta 2000). Fluoride is an essential element for maintaining normal development of healthy teeth and bones. However, higher F<sup>-</sup> concentration causes dental and skeletal fluorosis such as mottling of teeth, deformation of ligaments and bending of spinal chord. Concentration of F<sup>-</sup> exceeds the permissible limit of 1.5 mg L<sup>-1</sup> in about 37 % of the Jhansi groundwater samples. Concentrations of Cl<sup>-</sup> and SO<sub>4</sub><sup>2-</sup> are well within the desirable limit of 250 and 200 mg L<sup>-1</sup> respectively except at sites 1 and 63.

Among the cations, Na<sup>+</sup> is most important ions for human health. A higher sodium intake may cause hypertension, congenital heart diseases, nervous disorder and kidney problems. The recommended limit for sodium concentration in drinking water is 200 mg L<sup>-1</sup> (WHO 2006; BIS 2003). Concentrations of Na<sup>+</sup> are within the recommended limit of 200 mg L<sup>-1</sup> in Jhansi groundwater samples except at site 1.

Calcium and magnesium is an essential element for bone, nervous system and cell development. One possible adverse effect from ingesting high concentration of Ca<sup>2+</sup> for long periods may be an increased risk of kidney stones (Maragella et al. 1996). Concentration of Ca<sup>2+</sup> and Mg<sup>2+</sup> are exceeding the desirable limits of 75 and 30 mg L<sup>-1</sup> in 16 % and 46 % of the groundwater samples respectively. However, concentrations of both these ions are within the maximum permissible limit of 200 and 100 mg L<sup>-1</sup> except for Mg<sup>2+</sup> at sites 1 and 63 (BIS 2003). The trace metal analysis shows that except Fe, concentrations of the most of the analysed metals are well within the desirable levels prescribed for the drinking water (BIS 2003).

#### Suitability for irrigation uses

Water quality, soil types and cropping practices play an important role in assessing the suitability of water for irrigation. Total salt concentration (EC), sodium adsorption ratio (SAR), sodium percentage (Na %), residual sodium carbonate (RSC), Kelley index, permeability index (PI) and magnesium hazard (MH) are the important parameters which are widely used in assessing the suitability of water for irrigation uses (Ayers and Westcot 1985). Electrical conductivity and sodium concentration are very important in classifying irrigation water. The high salts in the water, besides affecting the growth of the plants directly, also affect the soil structure, permeability and aeration, which indirectly affect the plant growth. The U. S. Salinity Laboratory (1954) proposed a diagram for studying the suitability of groundwater for irrigation purposes based electrical conductivity and sodium adsorption ratio (SAR). In this diagram, irrigation water are classified as low (EC = <250 μS cm<sup>-1</sup>), medium (250–750 μS cm<sup>-1</sup>), high (750–2,250 μS cm<sup>-1</sup>) and very high (2,250–5,000 μS cm<sup>-1</sup>) salinity classes (USSL 1954). High salt concentration in water leads to formation of saline soil, while a high sodium concentration leads to development of an alkaline soil. The sodium or alkali hazard expressed in terms of sodium adsorption ratio (SAR) and estimated by the formula:

$$\text{SAR} = \frac{\text{Na}^+}{\sqrt{(\text{Ca}^{2+} + \text{Mg}^{2+})/2}}$$

all concentrations in meq L<sup>-1</sup>

On the basis of SAR value, water are classified into low (SAR <6), medium (6–12), high (12–18) and very high (>18) alkali waters. There is a significant relationship between SAR values of irrigation water and the extent to which sodium is adsorbed by the soils. If water used for irrigation is high in sodium and low in calcium, the cation-exchange complex may become saturated with sodium.

This can destroy the soil structure owing to dispersion of the clay particles. The calculated value of SAR in the groundwater of Jhansi district ranges from 0.29 to 9.05 (avg. 1.83) and the data plotted on the USSL diagram fall in the category of C2S1 and C3S1. Medium salinity and low alkali water (C2S1) can be used for irrigation in most soil and crops with little danger of development of exchangeable sodium and salinity (Fig. 10a). About 15 % of the groundwater samples falling in the zone of C3S1 indicate high salinity and low alkali water. High saline water is not suitable for soils with restricted drainage and it requires a special management for salinity control.

Percent sodium (%Na) is another parameter which are widely used in evaluating the suitability of water for irrigation purposes. The sodium percentage (%Na) can be determined by the formula:

$$\%Na = \frac{Na + K}{Ca + Mg + Na + K} \times 100,$$

where all concentrations are in meq L<sup>-1</sup>.

Irrigation with high sodium water causes exchange of Na<sup>+</sup> in water for Ca<sup>2+</sup> and Mg<sup>2+</sup> in soil and reduces the permeability and eventually results in soil with poor internal drainage (Collins and Jenkins 1996). As per the Indian Standard maximum %Na of 60 % is recommended for irrigation water (BIS 2003). The %Na value in the Jhansi groundwater ranges between 8.8 and 84.2 % (avg. 33 %) and plot of analytical data on the Wilcox (1955) diagram show that groundwater of the study area is excellent to good and good to permissible quality for irrigation uses. Four groundwater samples fall in the zone of permissible to doubtful category and one in the unsuitable category (Fig. 10b).

The quantity of bicarbonate and carbonate in excess of alkaline earths (Ca<sup>2+</sup> + Mg<sup>2+</sup>) also influence the suitability of water for irrigation purposes. The excess of CO<sub>3</sub><sup>2-</sup> + HCO<sub>3</sub><sup>-</sup> over Ca<sup>2+</sup> + Mg<sup>2+</sup> may cause complete precipitation of Ca<sup>2+</sup> and Mg<sup>2+</sup> as carbonate (Karanth 1989). The effect of carbonate and bicarbonate and suitability of water for irrigation can be assessed by computing the residual sodium carbonate (RSC) values by the following formula:

$$RSC = (CO_3^{2-} + HCO_3^-) - (Ca^{2+} + Mg^{2+})$$

all concentration in meq L<sup>-1</sup>

A high value of RSC in water leads to an increase in the adsorption of sodium on soil (Eaton 1950). Irrigation waters having RSC values greater than 5 meq L<sup>-1</sup> have been considered harmful to the growth of plants, while waters with RSC values above 2.5 meq L<sup>-1</sup> are unsuitable for irrigation. A RSC value between 1.25 and 2.5 meq L<sup>-1</sup> is considered as the marginal quality and value <1.25 meq L<sup>-1</sup> as the safe limit for irrigation. The calculated

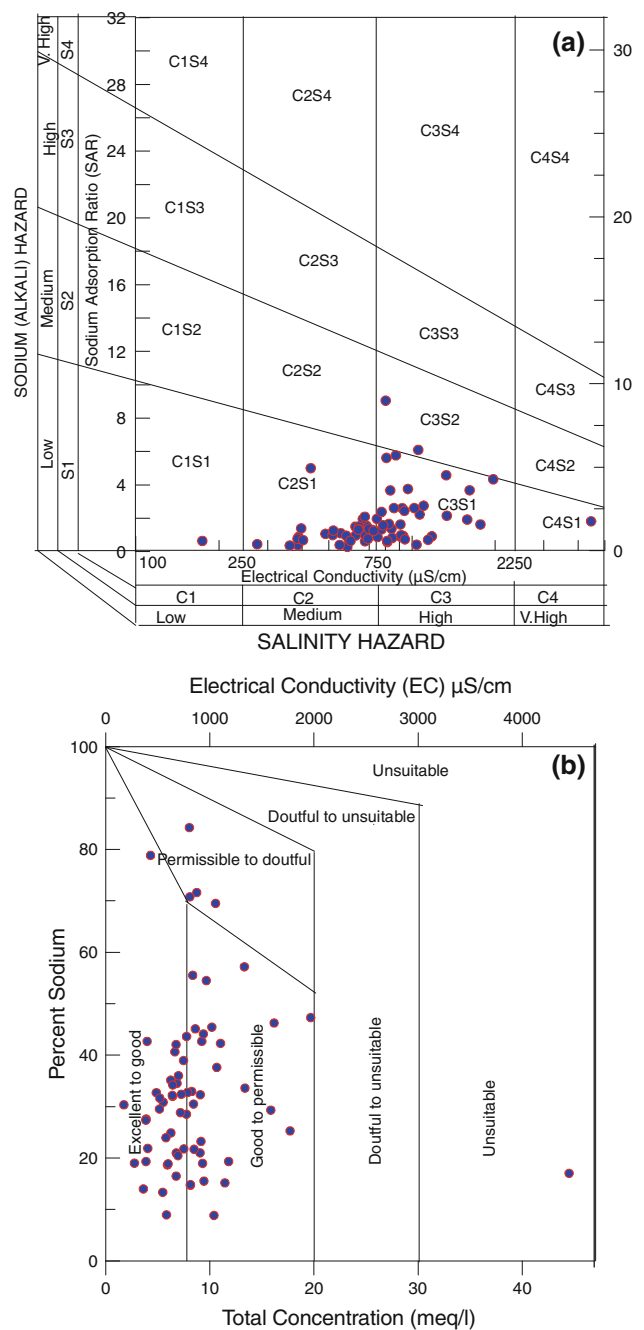


**Fig. 10** a US Salinity Laboratory, and b Wilcox diagrams for the classification of irrigation water

RSC values in the groundwater ranges between -25 and 8.4 meq L<sup>-1</sup> (avg. 0.63 meq L<sup>-1</sup>) and in about 20 % of the groundwater samples, it exceeded the 2.5 meq L<sup>-1</sup> limit, making the water as safe to marginally suitable category for irrigation uses (Table 1).

Kelley (1946) proposed an index (KI) to classify water for irrigation uses. Kelley’s index is the ratio of Na<sup>+</sup> / (Ca<sup>2+</sup> + Mg<sup>2+</sup>) and waters with a <1.0 Kelley’s ratio are only considered suitable for irrigation. Kelley’s ratio in the

Jhansi groundwater varied from 0.09 to 5.33 (avg. 0.65) and 88 % of the samples having KI value below 1.0, suggesting that water is suitable for irrigation (Table 1). The KI value exceeded the specified limit (KI >1.0) in eight groundwater samples, making it unsuitable for irrigation use.

## Conclusions

The groundwater of the Jhansi districts is mildly acidic to alkaline in nature.  $\text{Ca}^{2+}$ ,  $\text{Mg}^{2+}$  and  $\text{Na}^+$  dominate hydrochemistry of the groundwater in cationic concentrations and  $\text{HCO}_3^-$  and  $\text{Cl}^-$  in anionic abundances. In the majority of the groundwater samples, concentrations of alkaline earths ( $\text{Ca}^{2+} + \text{Mg}^{2+}$ ) exceed alkali cations ( $\text{Na}^+ + \text{K}^+$ ) and  $\text{HCO}_3^-$  dominate over ( $\text{SO}_4^{2-} + \text{Cl}^-$ ).  $\text{Ca}^{2+}$ – $\text{Mg}^{2+}$ – $\text{HCO}_3^-$  and  $\text{Na}^+$ – $\text{HCO}_3^-$  are the dominant hydrogeochemical facies. Water chemistry of the study area strongly reflects the dominance of weathering of rock forming minerals with secondary inputs from anthropogenic and atmospheric sources. The high contribution of ( $\text{Ca}^{2+} + \text{Mg}^{2+}$ ) to the total cations, relatively high ( $\text{Na}^+ + \text{K}^+$ )/TZ<sup>+</sup> ratio (0.33) and low equivalent ratio of ( $\text{Ca}^{2+} + \text{Mg}^{2+}$ )/( $\text{Na}^+ + \text{K}^+$ ) i.e. 2.8 suggest that the chemical composition of the water is largely controlled by silicate weathering with limited contribution via carbonate weathering. The saturation indices of calcite (SI<sub>c</sub>) and dolomite (SI<sub>d</sub>) demonstrate that most of the groundwater samples are oversaturated with respect to dolomite and calcite, signifying the presence of calcareous nodules in the sub-surface soil profile of the area. In majority of the samples, the analyzed parameters are well within the desirable limits and water is potable for drinking purposes. However, concentrations of TDS, TH,  $\text{NO}_3^-$ ,  $\text{F}^-$ ,  $\text{Ca}^{2+}$ ,  $\text{Mg}^{2+}$  and Fe exceeds the desirable limit at few sites and require treatment before its utilization. Suitable water treatment process such as water softening, ion exchange and demineralization may be used to reduce the concentrations of contaminants. Quality assessment for irrigation suitability suggests excellent to good category of Jhansi groundwater, which can be, used for irrigation without any serious hazards. High salinity and residual sodium carbonate value at few sites restricts the suitability of groundwater for agricultural purposes and demands special management plan.

**Acknowledgments** Authors are grateful to Dr. A. Sinha, Director, Central Institute of Mining and Fuel Research for his kind support and permission to publish this paper. Financial support by the Council of Scientific and Industrial Research (CSIR), New Delhi under its 11th Five Year Plan Project (IAP-006) is gratefully acknowledged. We thank Dr. B. K. Tewary and other laboratory colleagues for their support and encouragement.

## References

- Agrawal V, Jagetia M (1997) Hydrogeochemical assessment of groundwater quality in Udaipur city, Rajasthan, India. In: Proceedings of national conference on dimension of environmental stress in India, Department of Geology, MS University, Baroda, India
- Alemayehu T, Dietzel M, Leis A (2010) Geochemical evolution of groundwater quality in shallow and deep wells of volcanic aquifer in Axum, Ethiopia. In: Proceedings of XXXVIII IAH Congress, Krakow-Poland
- Andre L, Franceschi M, Pouchan P, Atteia O (2005) Using geochemical data and modeling to enhance the understanding of groundwater flow in a regional deep aquifer, Aquitaine Basin, south-west of France. *J Hydrol* 305:40–62
- APHA (1998) Standard methods for the examination of water and waste water, 20th edn. American Public Health Association, Washington, DC
- Appelo CAJ, Postma D (1996) Geochemistry, groundwater and pollution. AA Balkema Publishers, Rotterdam
- Ayers RS, Westcot DW (1985) Water quality for irrigation. FAO Irrigation and Drainage Paper No. 20, Rev 1, FAO Rome
- Basu AK (1986) Geology of parts of the Bundelkhand Granite Massif, Central India. *Rec Geol Sur India* 117:61–120
- Berner EK, Berner RA (1987) The global water cycle: geochemistry and environment. Prentice-Hall, Englewood Cliffs
- BIS (2003) Indian standard drinking water specifications IS 10500:1991, edition 2.2 (2003–2009), Bureau of Indian Standards, New Delhi
- Bradon C, Homman K (1995) The cost of inaction: valuing the economy-wide cost of environmental degradation in India. Asia Environment Division, World Bank 7, October memo
- Cerling TE, Pederson BL, Damm KLV (1989) Sodium-calcium ion exchange in the weathering of shales: implication for global weathering budgets. *Geology* 17:552–554
- CGWB (2008) Groundwater brochure of Jhansi district, Uttar Pradesh. Central Ground Water Board, New Delhi
- Choubisa SL (2001) Endemic fluorosis in southern Rajasthan, India. *Fluoride* 34:61–70
- Collins R, Jenkins A (1996) The impact of agricultural land use on stream chemistry in the middle hills of the Himalayas, Nepal. *J Hydrol* 185:71–86
- Datta PS, Tyagi SK (1996) Major ion chemistry of groundwater of Delhi area: chemical weathering processes and groundwater flow regime. *J Geol Soc India* 47:179–188
- Demlie M, Wohnlich S, Wisotzky F, Gizaw B (2007) Groundwater recharge, flow and hydrogeochemical evolution in a complex volcanic aquifer system, Central Ethiopia. *J Hydrogeol* 15:1169–1181
- Deutsch WJ (1997) Groundwater geochemistry: fundamentals and application to contamination. CRC Press, Boca Raton
- Durvey VS, Sharma LL, Saini VP, Sharma BK (1991) Handbook on the methodology of water quality assessment. Rajasthan Agricultural University, India
- Eaton FM (1950) Significance of carbonates in irrigation waters. *Soil Sci* 39:123–133
- Fisher RS, Mullican WF (1997) Hydrochemical evolution of sodium sulphate and sodium chloride groundwater beneath the Northern Chihuahuan desert, Trans-Pecos, Texas, USA. *Hydrogeol J* 5:4–16
- Freeze RA, Cherry JA (1979) Groundwater. Prentice-Hall, Englewood Cliffs
- Gaillardet J, Dupre B, Louvat P, Allegre CJ (1999) Global silicate weathering and CO<sub>2</sub> consumption rates deduced from the chemistry of large rivers. *Chem Geol* 159:3–30

- García MG, del v Hidalgo M, Blessa MA (2001) Geochemistry of groundwater in the alluvial plain of Tucuman province, Argentina. *Hydrogeol J* 9:597–610
- Garrels RM, Christ CL (1965) Solutions, minerals and equilibria. Harper and Row, New York
- Garrels RM, Mackenzie FT (1971) Gregor's denudation of the continents. *Nature* 231:382–383
- Ghosh A (2007) Current knowledge on the distribution of arsenic in groundwater in five states of India. *J Environ Sci Health Part A* 42:1–12
- Gibbs RJ (1970) Mechanisms controlling world water chemistry. *Science* 17:1088–1090
- Hounslow AW (1995) Water quality data: analysis and interpretation. CRC Lewis Publishers, New York
- Jalali M (2007) Assessment of the chemical components of Famenin groundwater, western Iran. *Environ Geoch Health* 29:357–374
- Jha SK, Shrivastava JP, Bhairam CL (2012) Clay mineralogical studies on Bijawars of the Sonrai basin: palaeoenvironmental implications and inferences on the uranium mineralization. *J Geol Soc Ind* 79:117–134
- Karant K (1989) Groundwater assessment development and management. Tata McGraw-Hill Publishing Company Ltd, New Delhi
- Kelley WP (1946) Permissible composition and concentration of irrigation waters. In: *Proceeding American Society of Civil Engineering*
- Kumar R, Singh RD, Sharma KD (2005) Water resources of India. *Curr Sci* 89:794–811
- Majumdar D, Gupta N (2000) Nitrate pollution of groundwater and associated human health disorders. *Indian J Environ Hlth* 2:28–39
- Maragella M, Vitale C, Petrarulo M, Rovera L, Dutto F (1996) Effects of mineral composition of drinking water on risk for stone formation and bone metabolism in idiopathic calcium nephrolithiasis. *Ciln Sci* 91:313–318
- McLean W, Jankowski J, Lavitt N (2000) Groundwater quality and sustainability in an alluvial aquifer, Australia. In: Sililo O et al (eds) *Groundwater, past achievements and future challenges*, Balkema, Rotterdam
- Mishra RC, Sharma RP (1975) Petrochemistry of Bundelkhand complex of central India. *Indian Mineral* 15:43–50
- Piper AM (1944) A graphical procedure in the geochemical interpretation of water analysis. *Trans Am Geoph Union* 25:914–928
- Rao AS, Srinivasarao C, Srivastava S (2011) Potassium status and crop response to potassium on the soils of agroecological regions of India. International Potash Institute, Switzerland
- Reddy DV, Nagabhushanam P, Perters E (2011) Village environs as source of nitrate contamination in groundwater: a case study in basaltic geo-environment in central India. *Environ Monit Assess* 174:481–492
- Rose (2002) Comparative major ion geochemistry of piedmont streams in the Atlanta, Georgia region: possible effects of urbanization. *Environ Geol* 42:102–113
- Sarin MM, Krishnaswamy S, Dilli K, Somayajulu BLK, Moore WS (1989) Major ion chemistry of the Ganga-Brahmaputra river system: weathering processes and fluxes to the Bay of Bengal. *Geochim Cosmochim Acta* 53:997–1009
- Sawyer CN, McCarty PL (1967) *Chemistry of sanitary engineers*, 2nd edn. McGraw Hill, New York
- Schoeller H (1977) Geochemistry of groundwater. In: *Groundwater studies—an international guide for research and practice*, Ch. 15. UNESCO, Paris, pp 1–18
- Singh AK, Mondal GC, Singh PK, Singh S, Singh TB, Tewary BK (2005) Hydrochemistry of reservoirs of Damodar River basin, India: weathering processes and water quality assessment. *Environ Geol* 48:1014–1028
- Singh AK, Mondal GC, Kumar S, Singh TB, Tewary BK, Sinha A (2008) Major ion chemistry, weathering processes and water quality assessment in upper catchment of Damodar River basin, India. *Environ Geol* 54:745–758
- Singh AK, Tewary BK, Sinha A (2011) Hydrochemistry and quality assessment of groundwater in part of NOIDA metropolitan city, Uttar Pradesh. *J Geol Soc India* 78:523–540
- Srikanth R (2009) Challenges of sustainable water quality management in rural India. *Curr Sci* 3:317–325
- Stumm W, Morgan JJ (1981) *Aquatic chemistry*. Wiley Interscience, New York
- Subramanian V (2000) *Water: quantity-quality perspectives in South Asia*. Kingston International Publishers Ltd, Surrey
- Susheela AK (1999) Fluorosis management programme in India. *Curr Sci* 77:1256–1259
- Susheela AK, Kumar A, Bhatnagar M, Bahadur M (1993) Prevalence of endemic fluorosis with gastrointestinal manifestations in people living in some north-Indian villages. *Fluoride* 26:97–104
- Taylor SR, MacLennan SM (1985) *The continental crust: its composition and evolution*. Blackwell, Oxford
- Teotia SPS, Teotia M (1984) Endemic fluorosis in India: challenging national health problem. *J Assoc Phys India* 32:347–352
- USSL (US Salinity Laboratory) (1954) *Diagnosis and improvement of saline and alkali soils*. US Department of Agriculture Hand Book, No 60
- Vidal M, Melgar J, Opez AL, Santoalla MC (2000) Spatial and temporal hydrochemical changes in groundwater under the contaminating effects of fertilizers and wastewater. *J Environ Manage* 60:215–225
- WHO (2006) *Guidelines for drinking-water quality*, vol 1, Recommendations, 3rd edn. World Health Organization, Geneva
- Wilcox LV (1955) *Classification and use of irrigation waters*. US Department of Agriculture, Circular 969, Washington, DC, USA
- Zhang J, Huang WW, Letolle R, Jusserand C (1995) Major element chemistry of the Huanghe (Yellow river), China—weathering processes and chemical fluxes. *J Hydrol* 168:173–203